ILLEGIB

HIGH PRECISION STEREO COMPARATOR STUDY

MONTHLY NARRATIVE REPORT

FOR PERIOD ENDING OCTOBER 1, 1965

Approved For Release 2003/05/15 : CIA-RDP78B04747A002700040006-3

FOREWORD

The first five sections of this report summarize the effort and conclusions reached during the reporting period. The appendices provide detailed information and analyses to justify the conclusion. It is expected that the appendices in this and other monthly summaries will furnish the basis for the final engineering report.

TABLE OF CONTENTS

TABLE OF CONTENTS

STAT
STAT

TABLE OF CONTENTS

LIST OF ILLUSTRATIONS

LIST OF ILLUSTRATIONS

STAT

1.0 CURRENT STATUS OF WORK

1.1 Optical System

The definition of the visual observation system is now complete through the light source, condenser optics, objective turret, image rotator, and reticle dot, except for establishment of some of the alignment and positioning tolerances. The method of integrating a scanner system (for automatic correlation) has also been defined and the light-collecting optics for a photomultiplier have been integrated with the condenser system.

The work on the optical switch which had been scheduled for completion in September was postponed in order to complete the above-mentioned subsystems, which have a much greater impact on the mechanical design.

Detailed descriptions of the optical subsystems are contained in Appendices A, B, and C.

1.2 Mechanical

Configuration design of the X-Y measuring stages and optics framework proceeded during the reporting period. Stress and deflection calculations are now in progress to determine the basic sections sizes.

Layout of the objective turret, image rotator and reticle dot assembly was started during the reporting period. It is expected to be complete early in November.

STAT

A final material selection for the precision stages has not yet been made. Appendix G contains a discussion of the three most likely materials: meehanite cast iron, 410 stainless steel, and granite. In the case of meehanite a problem of corrosion protection exists. It appears that either a chrome flash or an electroless nickel deposit may be suitable if build-up can be controlled, and vendors are being contacted to determine their capability for handling the anticipated large castings.

1.3 Correlation

1.3.1 Electronic Analog Correlator

The circuitry for the analog correlation is now complete and has been tested on simulated input signals. In particular, the ability to show degree of correlation between sine waves of different phase throughout the design bandwidth (50 KC to 5 MC) has been demonstrated. A description of the theory of operation and circuit design is contained in Appendix E.

1.3.2 Electronic Digital Correlator

As previously reported, tests of this correlator are scheduled to start in October.

1.3.3 Electro-Optical Correlator

The equipment modifications described in the previous report have proceeded. A full description of this correlation system is contained in Appendix D.

1.4 Metering System

STAT

The demonstration verified that the system repeatability was as

claimed, and that over a limited range several gage blocks were measured with a high degree of accuracy. The [redacted] system is not to be developed into a standard package and therefore it would be necessary to design its components into the mechanism of the Stereo Comparator. This, of course, would also be true of the laser interferometer discussed in last month's report. During October drawings will be prepared to show how each of these systems would be integrated into the X-Y stages.

STAT

A description and comparison of the [redacted] metering system is contained in Appendix

STAT

1.5 General System Considerations

1.5.1 Overall Format Observation

During the reporting period efforts were continued to devise a technique to permit convenient viewing of the overall format. The two major criteria were that the technique not require generation of expendable hard copies of the input photography, and that the display must maintain very high quality (good resolution, brightness and grey-scale) for indefinite periods of time. In addition the technique must not add to the complexity of operation or significantly reduce the speed of operation.

The first criterion rules out photocopying, diazo copying, etc., and requires the consideration of reversible information storage systems. Among those considered were: Photochromic dyes, magnetic tape and drums, image storage tubes, thermoplastics, reversible Xerography, and electroluminescent displays.

As mentioned in the second monthly report, no photochromic or electroluminescent systems are known which will maintain image quality over protracted times, particularly at room temperature. The same is true of image storage tubes, with the possible

exception of a special tube [redacted] which uses an auxiliary light source within the tube to illuminate an image produced by electron beam writing on a special face material. However, the [redacted] tube requires repeated writing in order to attain a satisfactory grey scale. Also, erasure requires five to ten seconds, so that both writing and erasing are incompatible with system timing requirements. STAT STAT

A trip was made [redacted] to discuss the practicality of a reversible [redacted] process, achieved by omitting the normal fixing operation. It was established that the technique was probably feasible, and that such a system would not require extensive development. However, in its basic form [redacted] they could guarantee no more than five shades of grey, which does not sound acceptable. STAT STAT STAT

[redacted] working on a thermoplastic process which they call "FROST", which may have promise for the future, but it is not expected to be available during the course of the Stereo Comparator program. STAT

There are three principal companies engaged in the manufacture of video recording equipment [redacted] They have been surveyed to determine the practicality of using a magnetic tape or drum to store the picture information, with a "stop motion" feature to permit continuous display of any given frame. STAT

[redacted] STAT

a letter from their representative advises that more than 2 1/2 hours has been achieved. The cause of the loss of picture is not entirely clear from conversations with them, but it is believed to be a combination of abrasion of the tape surface and fouling of the head gap, accelerated by heat build-up due to repeated rubbing over the same tape section [redacted] that actual head-to-tape contact is necessary in video recording.) STAT

[redacted] successfully used a special lubricant which apparently permits indefinitely extended re-play. However, although the lubricant provides successful tape protection they caution strongly against its use unless absolutely necessary, because of the probability of harmful accumulations throughout the recorder mechanism. STAT

At the present time a proposal is expected [redacted] for a system incorporating a magnetic drum and multiple read-write heads which is claimed to have satisfactorily high life and the capability of continuous scanning or display of any part of the stored video data. Extensive system integration problems are foreseen, however, and a search is continuing for more acceptable solutions. STAT

2.0 PROBLEM AREAS

2.1 Optical

No new problems are apparent in this area. Tolerance requirements will be a continuing concern until they are completely defined.

Resolution requirements still appear to be attainable, and it is planned to obtain confirmation of the soundness of the system approach by discussions with potential vendors in the fifth month of the program.

2.2 Mechanical

Work on the film transport mechanism has had to be temporarily suspended because of more interaction than had been expected between the optical design and the transport configuration. This is particularly true of the small working space now predicted for the highest power objective lens, which complicates transport removal, and the very shallow depth of field similarly predicted. The transport design will be resumed when this data is definitized.

Tests of vacuum hold-down systems have been suspended pending receipt of representative film samples covering the range of film thicknesses and widths expected. These samples were requested from contracting office personnel at their last visit to [redacted] STAT

The X-Y comparator stages and optical frame designs are proceeding satisfactorily and no technical impossibilities are apparent at present. The massiveness of the tables is such that careful placement within the allotted room will be necessary. Information is needed regarding the arrangement of building services (air, power, and ventilation) within this room, as well as the location of doorways.

2.3 Correlation

No unforeseen technical problems.

2.4 Metering Systems

At the present time the choice for a metering system is seen as [redacted] Interferometer. On a technical basis the Interferometer, if properly used, is felt to provide a substantially higher accuracy capability, though it is questionable whether this potential can be usefully employed. [redacted] provides the greatest protection against miscounting. On the basis of budgetary estimates [redacted] appears to be significantly more expensive. The ease of application of either system will be more apparent after the current month's effort is completed.

STAT

STAT

STAT

Since some of these trade-offs are economic in nature, and others involve anticipated usage of the Comparator, a final recommendation will not be made until after further discussions with the Contracting Office.

2.5 General Systems

The presentation of the overall format display has always been regarded as a critically important aspect of the Comparator operation. The problem has proven much more difficult than originally expected and no really satisfactory technique has been conceived to date.

It is hoped that new inputs [redacted] in the next month will contribute toward a solution to the display requirement. If not, serious consideration will be given to several possible hybrid combinations of short-term and long-term storage and display systems. These have been considered casually in the course of the study, but have not been reported previously because of their objectionable complexity and probable high cost.

STAT

3.0 PROJECTED WORK FOR NEXT REPORTING PERIOD

3.1 Optical

Design will continue on the zoom and relaying system. It is hoped that all critical elements will be complete by mid-November so that the design can be presented to potential vendors in time to take into consideration any recommended changes.

3.2 Mechanical

Casting configuration drawings for the X-Y stages and optical frames will be completed in October. Structural analysis will continue. Estimated weights of the stages will be available so that drive system design can be started.

3.3 Correlation

Data-taking on correlator performance is expected to begin in October.

3.4 Metering

Drawings showing integration of the two preferred systems will be prepared. Final selection will await discussions with the Contracting Office.

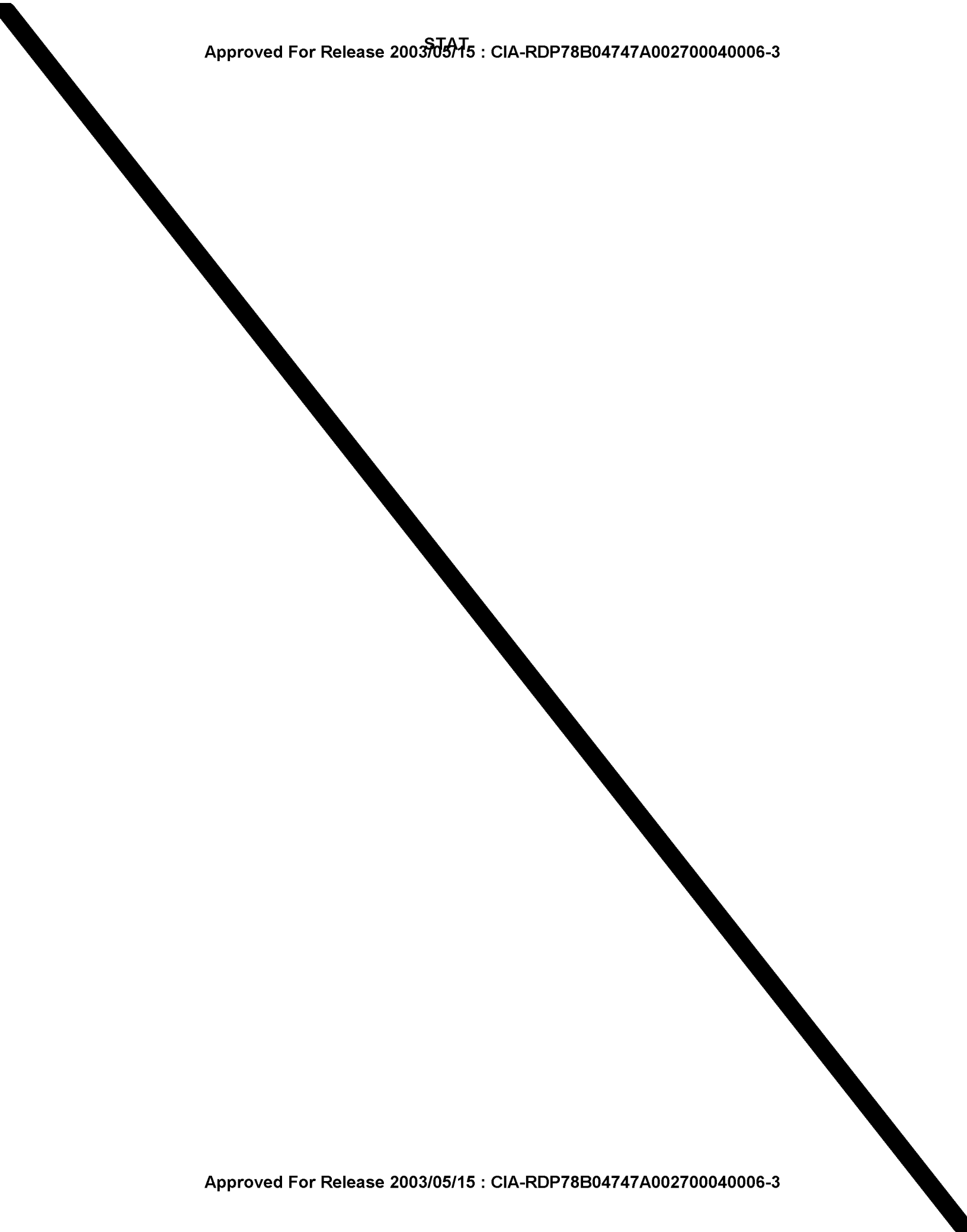

5.0 VERBAL COMMITMENTS AND AGREEMENTS

The Contracting Office has been requested to supply samples of film and, if possible, stereo photography to be used in forthcoming tests. Blank or exposed film is needed to perform tests on the hold-down system, and the samples should cover as wide a range of anticipated thicknesses and widths as possible. Stereo photography covering a spectrum of contrasts, scales, imagery and density would greatly facilitate correlator evaluation.

It is now understood that the requirement for theta alignment of the film has been eliminated, since computer corrections for misalignment are included in the data reduction program.

APPENDIX A

CONDENSER SUBSYSTEM

The image quality (resolution and "crispness") of an optical system resembling a microscope depends to a high degree upon the proper illumination. Both the object field and aperture diaphragm of the objective lens (exit pupil EX), have to be filled with light, the object field, of course, completely and EX to about three-fourths to four-fifths of its diameter. The latter is an empirical value which provides crispest image appearance. It is important to restrict the illumination light pencil to the necessary dimensions as early as possible along the optical train in order to avoid stray light, which will reduce contrast, and therefore severely impair image quality. This principle is best reduced to practice in the classical Koehler illumination scheme (see Figure A-1).

The condenser proper, Cond, is arranged immediately in front of the object plane, O.P. In its front focal plane, $\overline{F}$, is placed the aperture diaphragm, A.D., which serves as a secondary light source. The condenser, Cond, images A.D. into infinity in the object space. Since microscope objectives are telecentric lenses, i.e., their EX coincides with their back focal plane, A.D. is finally imaged into EX. Making A.D. an iris provides for its adjustment so that it fills three-fourths to four-fifths of Ex.

The filament of the light source, L.S., is imaged by a so-called collector, Coll., into the aperture diaphragm so that its structure is not noticeable in the object plane, O.P.. The optical components have to be dimensioned so that an iris behind the collector is imaged into O.P. by the condenser. This iris is then the field stop, F. St., which restricts the illumination to the required field size in O.P.

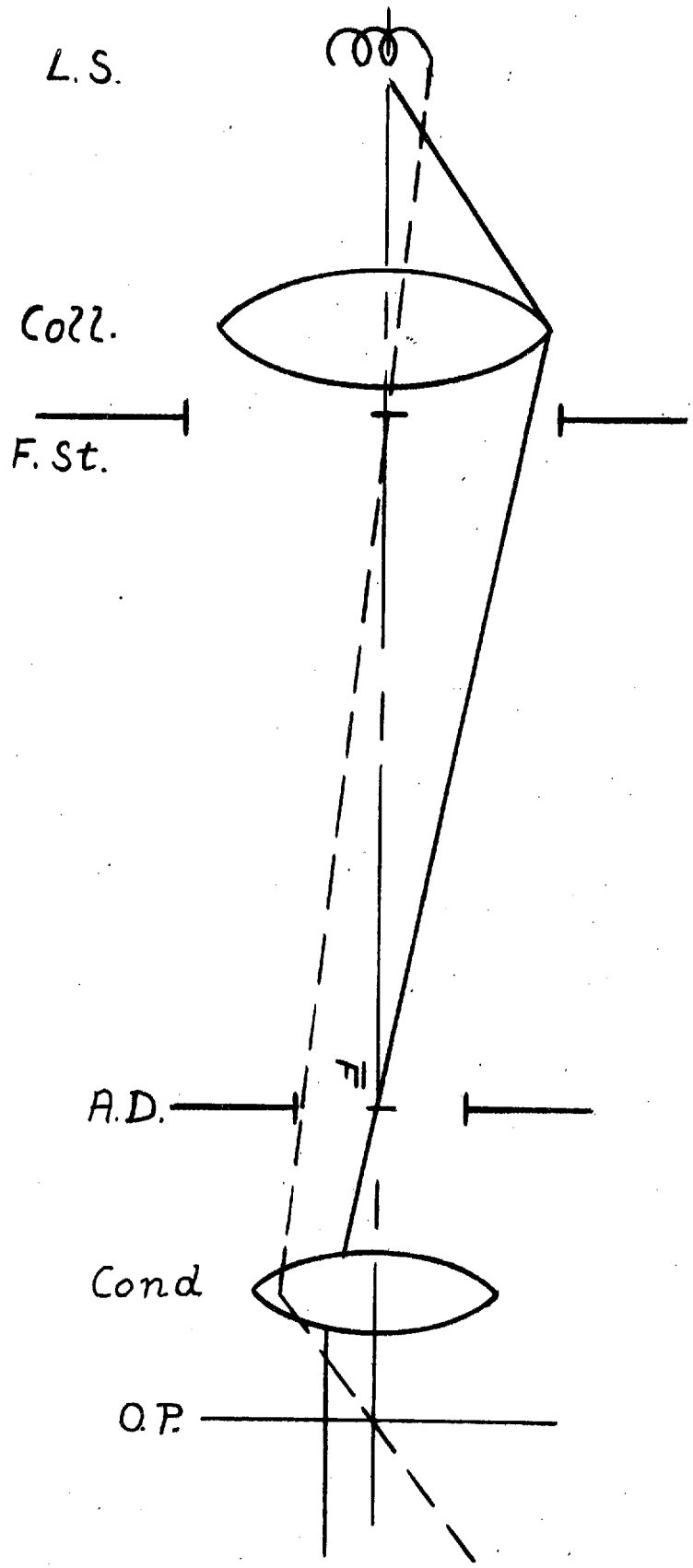

BASIC SCHEME OF KOEHLER ILLUMINATION

FIGURE A-1

Implementation of the Koehler-illumination for the Visual Observation System (VOS) is considered an absolute necessity for meeting the requirements of highest possible image quality. However, this implementation is difficult because of the large range of field size, from 18 to 0.861 mm diameter, and of numerical aperture, from 0.044 to 0.558 (see Appendix B, Table B-7). It is not possible to cover this large range without any change in the illumination system (besides the change of A.D. and F. St. diameters). An approach is used which is rather common in microscope design. The whole range is split into two parts, one for low magnification, large field and small N.A. (3.5x objective), and one for large magnification, small field and large N.A. (9x and 21x objectives).

The first approach for both cases (Figure A-2) is based on "thin lenses" and a paraxial ray trace using the formulas of Mil-Handbook 141 (Chapters 5 and 6):

$$n\,u = (n\,u)_{-1} - y\,F$$

$$y_{+1} = y + u\,t$$

$$F = (n-1)(c_a - c_b)$$

where: y = height of incidence at surface k under consideration.
u = slope angle behind surface k (in radians)
t = distance to next surface (k to k+1)
F = power of lens = $1/f$
f = focal length of lens
$c_a; c_b$ = lens curvature = $1/r_a$; $1/r_b$

This set of formulas is also known as "Lange lens formulas", the only difference between the Mil-Handbook 141 and conventional

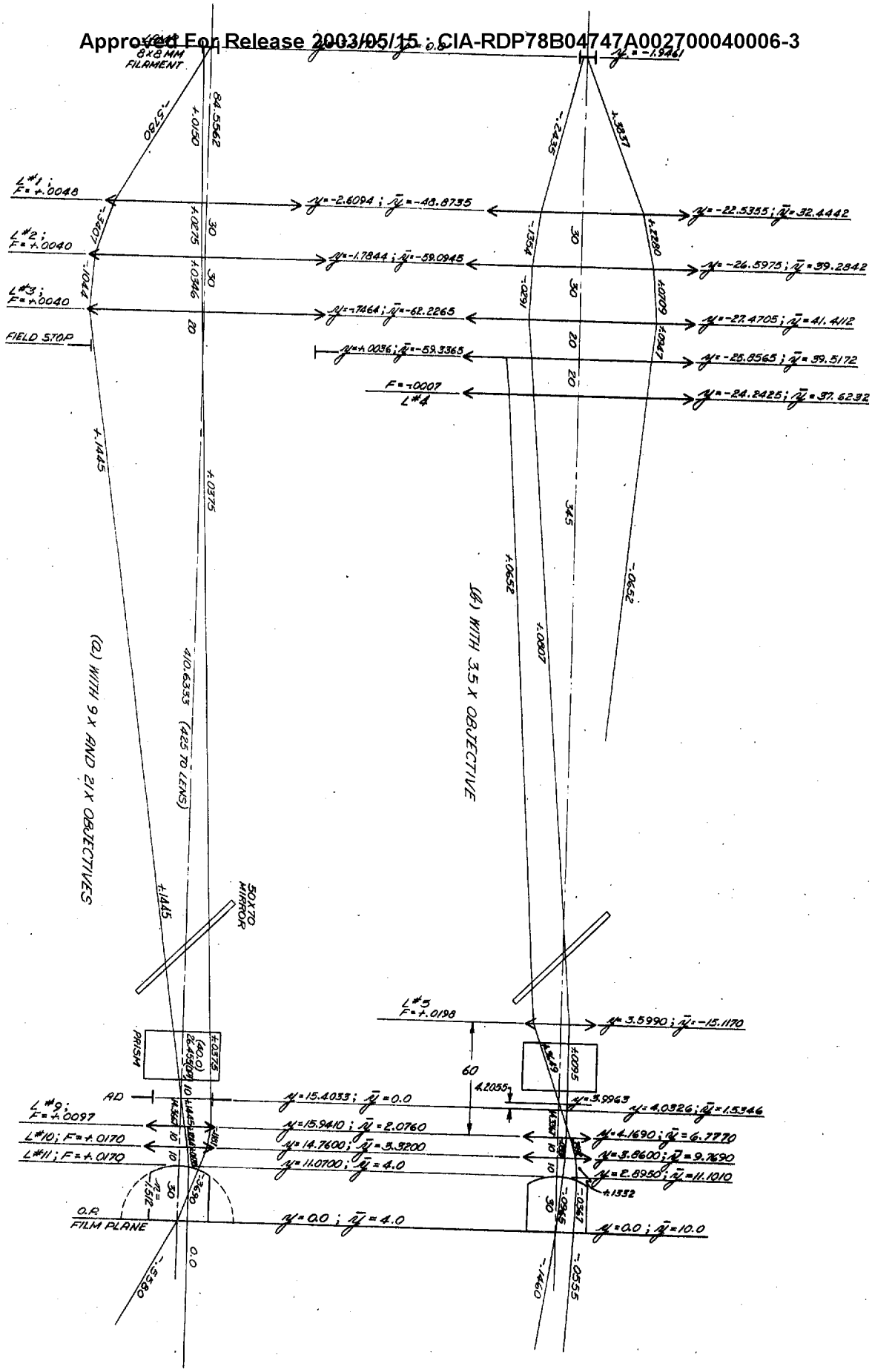

VOS ILLUMINATION SYSTEM

FIGURE A-2

textbooks being the difference of sign for u. The advantage of these formulas is that they avoid the reciprocals of the Gauss lens formula and that they permit direct use of important design parameters, namely, object and image size and numerical apertures.

The calculation proceeds backwards from the object plane with the maximum values for the 9x and 21x objectives: $\bar{y}' = 4.0$ for the chief "edge ray", i.e., the ray through the edge of the field (with a safety margin of 0.5 mm over the actual requirement) and $\bar{u} = 0.0$; N.A. = u = -.5580 for the "position" ray, i.e., the ray determining the position of the field (y = 0). The full maximum value for N.A. has been used though only three-fourths to four-fifths of the aperture should be filled with light, in order to have a safety margin.

The first lens of the condenser proper is, optically, a hemisphere following microscope design practice, because a hemisphere is "aplanatic", i.e., does not introduce spherical aberrations and coma. (This is important in view of the large aperture angle.) A small air gap within this lens is without consequence so that the glass plate for film support can be considered to be split off this hemisphere. It is important, however, to keep the overall glass thickness constant, and it must be maintained at the chosen value of 30 mm in the event that the platen is ever changed. This is unavoidable in view of the existing severe requirements. The angle at the air gap remains below the critical angle of total reflection, but it is advisable to coat the surface of lens L11 and the surface of the platen with a highly efficient and hard anti-reflection coating.

The next two lenses toward the light source, L10 and L9, bring the position ray back to the optical axis at a distance of 425 mm from L9, which determines the position of the field stop, F. St. This position is tentative; it can be increased without difficulty by decreasing the power of lens L9, if the mechanical table and condenser subassembly design should require such an increase. The chief ray intersects, then, the optical axis at a distance of 14.3667 mm from lens L9, which determines the position of the aperture diaphragm, A.D. The height of incidence of the position ray at this plane, y = 15.40 mm, determines the radius of the A.D. iris for the maximum N.A.

Next comes the first beamsplitter, "Prism". Its reduced thickness t/n (assumed n = 1.512) is given in Figure A-2 , thus making its consideration for the ray trace unnecessary. But it can be seen that a size of 40 by 40 mm suffices for this beamsplitter. A mirror is necessary to bend the optical axis back into the (approximately) original direction; its size is 50 by 70 mm. It can be used for the proper adjustment of the light direction with respect to mechanical design as well as for the shop assembly.

Between fieldstop and light source is the collector. It has to bring the chief ray back to the optical axis. The slope angle of the chief ray determines the magnification between light source and aperture diaphragm, and thus the required size of the filament, which should, of course, be as small as feasible. A slope angle u = -.578 is attainable, if a three lens collector is considered to be acceptable. This results in a magnification of m' = 4x and a filament size of 8 by 8 mm with a safety margin of 2 by 0.12 mm for the largest aperture in addition to the safety margin quoted above (use of the nominal value for the maximum N.A.).

A prospective choice for the lamp would be a [redacted] STAT lamp DFW or DGF, 500 w, 4 pin base, 25 hours life, 3200°K color temperature. Both have the compact type envelope and can be burnt horizontally as well as vertically. The average luminance is not quoted and information about it cannot be obtained (as usual, regrettably), but the filament is very compact (biplane) leaving only very small gaps between the coils so that the average luminance should be as high as possible. The difference between the two types is that DFW has a "proximity reflector" while DGF has none. Whether the proximity reflector (a reflector built into the lamp) has an advantage for this application must still be determined.

The filament size leaves practically no safety margin (8.0 x 7.8 mm). If it is too small a 750 w lamp such as the DEP has to be used (filament 9.4 x 9.6).

Of course, other manufacturers have similar lamps. Final choice will require some experiments, i.e., measurements in connection with the condenser, at least with the collector. The remarks about the lamp made here are only indicative of the type of lamp and the wattage required. Good forced cooling will always be a necessity in order to preserve lamp life and to avoid heating up of sensitive parts of the table by the lamp. Except for the most dense film it will be possible to reduce the lamp voltage and therefore extend its life.

It should be possible to handle the case of the 3.5x objective with the same lamp and general layout since the Lagrange (or "optical") constant ($OI = \bar{y}u - y\bar{u}$) is 1.460 (with $\bar{y}'(max) = 10.0$ mm and N.A. (max) = u = -.146) as compared to 2.22 for the 9x; 21x case. Some additional optical elements will be needed. The approach

taken [redacted] with its [redacted] condenser (removal of one condenser lens) should be avoided since it deviates from the Koehler-illumination principle. The filament structure then becomes noticeable in the image unless it is smeared out by a ground glass. The latter is not possible because it is accompanied by a considerable light loss which is intolerable for this application.

STAT
STAT

The field of 20.0 mm diameter (which includes a safety margin) results in an increase of the slope angle, $\bar{u}$, of the chief ray in the aperture diaphragm, namely $\bar{u}$ = + .3649 as compared to + .1445 in the previous case. This chief ray has to be brought back by a lens. The best choice for an additional "flip-in" lens is between beamsplitter "Prism" and "Mirror" (see Figure A-2). Its diameter would still be reasonably small, but $\bar{y}$ (for the chief ray) would still be large enough to have enough effect upon the chief ray with a reasonable lens power. The power of the lens, L_4, should be chosen so that the (new) chief ray intersects the former chief ray about 20 mm in front of the field diaphragm. A negative lens could be introduced in that place to restore the former optical train.

The power resulting for L5 is then F(5) = + .0162 (f = 62 mm). The power for the negative lens in front of F. St. would only be F = -.0007. This is so small that an attempt was made to omit it. Both the chief ray and the position ray intersect the plane of the lamp within the area of the filament, which is all that is required. The filament is then not exactly imaged into A.D., but this very small discrepancy is without any practical consequence within this context. Also, A.D. is not imaged absolutely

correctly into the EX of the 3.5x objective since EX does not coincide with the back focal plane of this lens, unlike the case of the 9x and 21x objectives. (This has been considered in the calculation by having $\bar{u}$ = .0555 instead of 0.0 in O.P.). But again, the discrepancy is so small that it can be neglected in this case.

However, the omission of L4 does produce an unfeasible design because the lens diameters for the collector lenses would have to be so large that this solution has to be considered unattainable. If the slope angle of the edge ray is made smaller (since it would suffice for a proper size of the filament image in the A.D. plane, namely .3837), the required filament size goes up, beyond that of the anticipated value of 8 by 8 mm.

The only way out is to start from the filament with a chief edge ray with $\bar{u}$ = + .3837 and to place a negative lens, L4, in front of the fieldstop, F. St. (a distance of 20 mm has tentatively been chosen), which bends the edge ray so that it hits lens L5 at the right height of incidence ($\bar{y}$ = -15.1170). The resulting lens powers are for L4, F = -.0007 and for L5, F = + .0198. Tracing the position ray through from L5 to the lamp results in a filament size of 4 by 4 mm, which is attainable.

It might be better to build the power of the negative lens L4 into the collector and to use a positive lens instead with the 9x, 21x objectives. The switch from the 9x, 21x case to the 3.5x case would thus involve removal of one lens and insertion of another. This might have advantages for the mechanical design. Optically, the advantage would be that there is a better chance to make lenses L2 and L3 equal, reducing their price, and use the (new) lens L4 for the correction of some aberrations. This favorable idea has

not been implemented at this stage of the development, since some more changes will have to be made after the mechanical design requirements have been established. The idea of such a change will, therefore, be left to the next design cycle; it will not change the basic design concept.

One disadvantage of this otherwise good approach is that F. St. will not be exactly correct for the 3.5x case. Its correct position would be near the front edge of the "Mirror" instead. Therefore there will be a small amount of excessive light in O.P. (a small diffuse zone of light around the edge of the field). This should have a negligible effect upon image quality in the 3.5x case since the 3.5x objective is rather far away and its numerical aperture is much smaller than the other.

The correlator case differs from the Visual Observation System (VOS) in that EX and, therefore, A.D. has to be imaged upon the photocathode, PM, without the necessity of having a defined fieldstop. (The image of the scanning spot in O.P. restricts the field sufficiently.) Also, the magnification between A.D. and PM will have to be larger, since a 2 inch diameter for the photocathode has been contemplated. But two cases still have to be considered: a) the 9x and 21x objectives and b) the 3.5x objective (see Figure A-3).

In the correlator case, one lens L7 will be common to a) and b). For a), lens L6 augments the power of lens L7 resulting in a maximum image size of A.D. (that is for the maximum N.A.) of $y = 20.2$ mm. Lens L6 is taken out and lens L8 is switched in for b). Lens L8 is again arranged near the beamsplitter prism and bends the chief ray toward lens L7. The maximum image size of A.D. on the photocathode is then $y = 10.6$ mm.

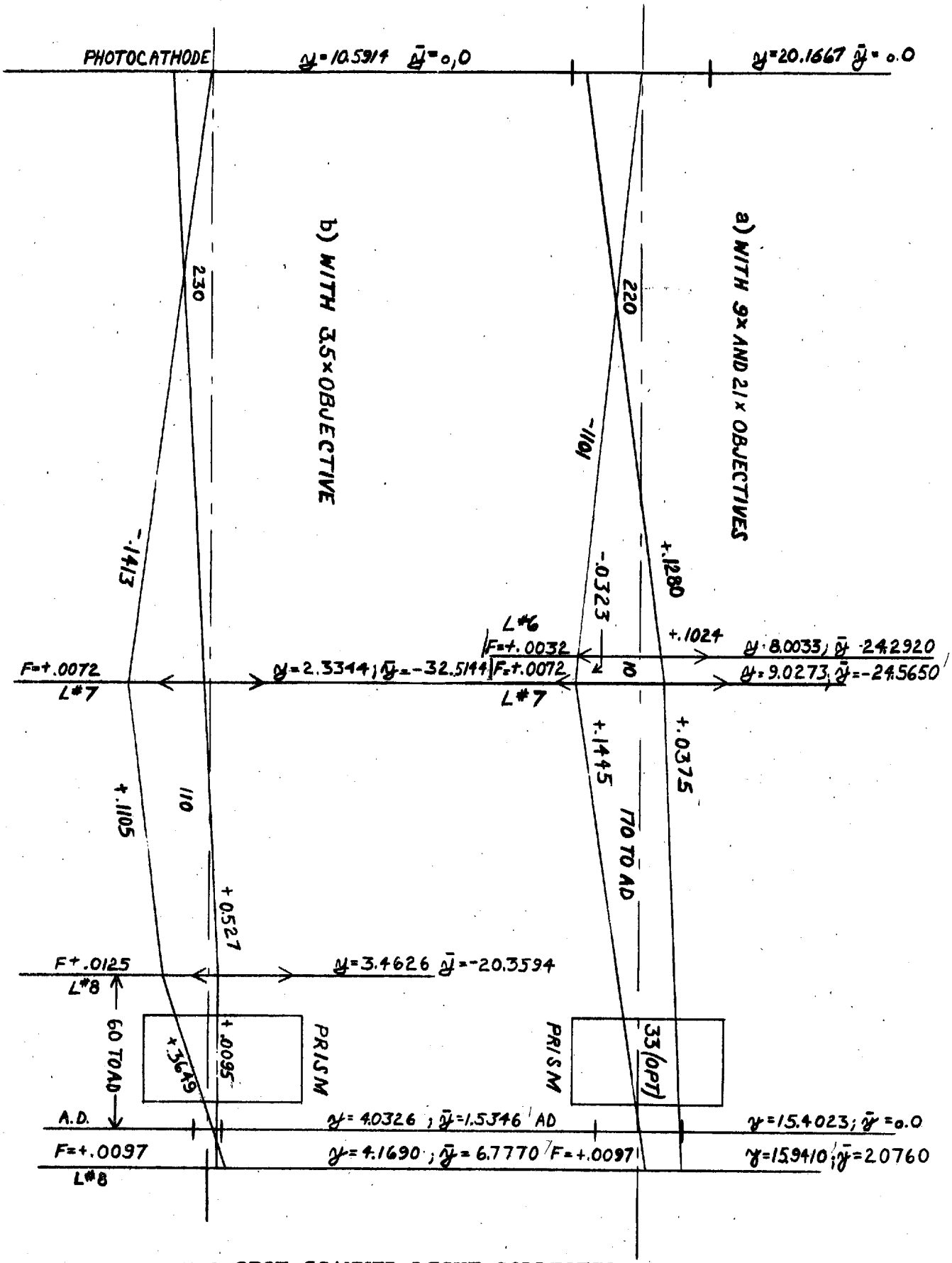

FLYING SPOT SCANNER LIGHT COLLECTION SYSTEM

FIGURE A-3

Both switch lenses, L6 and L8, can be attached to one axis of rotation since their optical axis coincides. This makes it possible to turn one lens in while the other lens is turned out.

A tentative mechanical arrangement for both optical trains (VOS and correlator, but for the 3.5x objective only) is shown in Figure A-4. It is necessary to bend the optical axis for the correlator train somewhat so that it does not interfere with the VOS train. Refraction by a small prism attached to the proper half of the beamsplitter should suffice for this purpose. Dispersion should not be a handicap since there is enough of a safety margin for y on the photocathode to take care of small image displacements because of dispersion.

One additional element will be required in the VOS train. It is necessary that the optical axis between lamp and collector be in an (approximately) horizontal position, even if the lamp is used in a horizontal position. Otherwise (that is if the optical axis runs vertically as shown in Figure A-4), blackening of the glass envelope above the filament by tungsten evaporation will soon spoil the brightness. This will make it necessary to use a plane mirror between table housing and collector, which makes it necessary to increase the distance of fieldstop and collector from the table housing. Since an optimum solution will have to result from the mechanical design, this problem has not been pursued further at the present.

Addition of the mirror will result only in a proportionately larger collector and a small power adjustment for the lenses L5 and L9. It will not change the general design concept, in particular, not the slope angle (N.A.) between lamp and collector and the filament (lamp) size. However, this situation makes it unadvisable

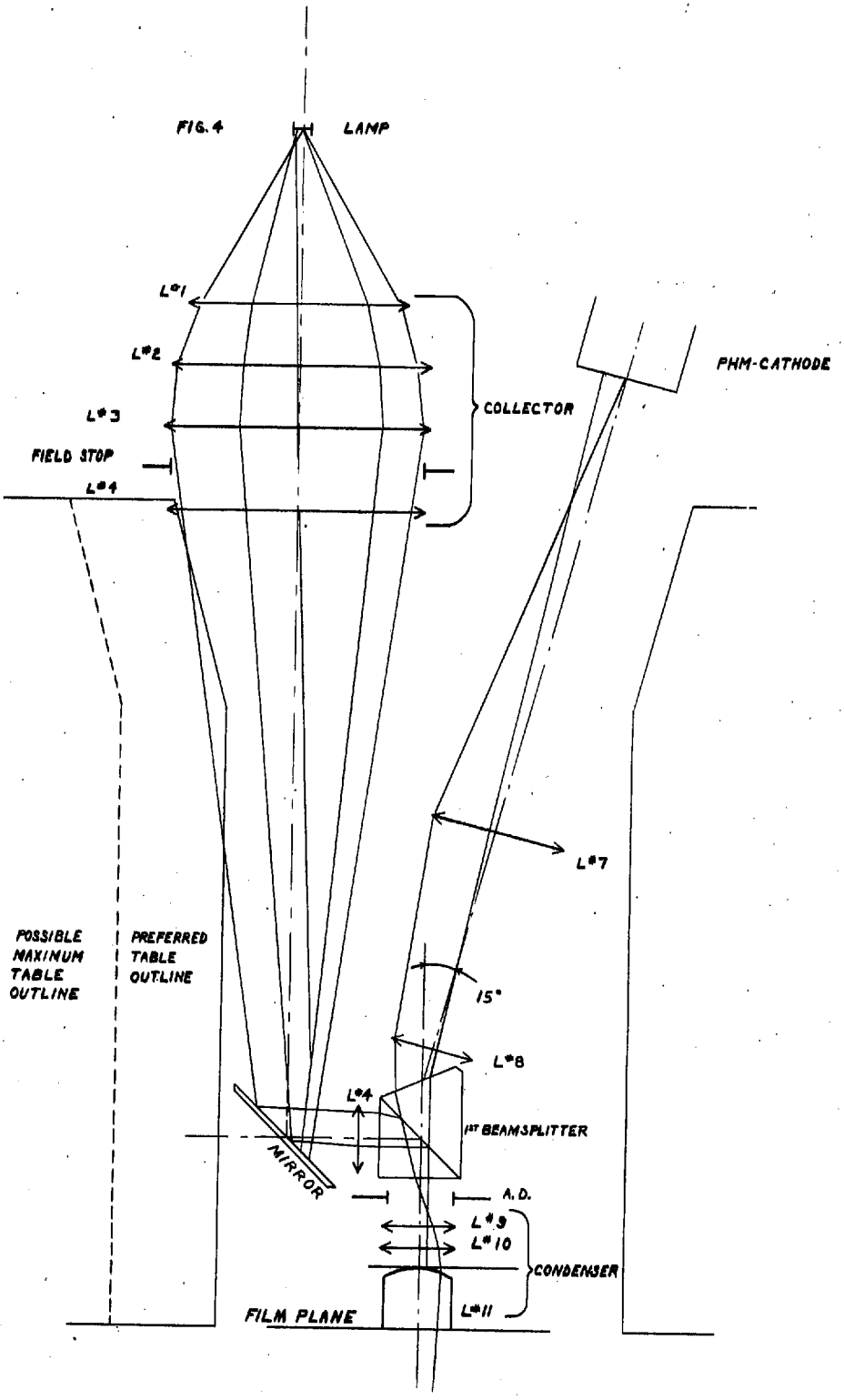

VOS CONDENSER & FSS COLLECTOR,
MECHANICAL ARRANGEMENT

FIGURE A-4

at this time to change the "thin" lenses into thick lenses and to determine their optimum shape from a (trigonometrical) ray trace. This task is routine work which should not cause severe difficulties so that it can be left for later.

Figure A-4 indicates that the condenser subsystem can be integrated in the table design without causing difficulties. Table A-1 lists all components for the condenser subassembly and their tentative dimensions. "Curvature" $c_a - c_b$ has been calculated from

$$c_a - c_b = F/(n-1); \; n = 1.512$$

and "estimated lens thickness", t_L, from

$$t_L \approx \frac{1}{8} D^2 (c_a - c_b).$$

Lens diameter D follows from the drawings (Figures A-2 and A-3) by

$$D \approx 2 (|y| + |\bar{y}|)$$

TABLE A-1

OPTICAL COMPONENTS FOR CONDENSER SUBASSEMBLY

Sub-Group	Component	Power $F[mm^{-1}]$	Focal Length f[mm]	Free Dia. D[mm]	Combined Curvature $c_a - c_b$ $[mm^{-1}]$	Estimated Thickness t_L[mm]*
VISUAL OBSERVATION SYSTEM (VOS)	Lamp: Biplane filament 8 x 8 mm, 500 or 750W					
	L1	+.0048	210	105	.0093	13
	L2; L3	+.0040	250	130	.0078	17
	Fieldstop, F.St., Iris Diaphragm, max. dia. = 120 mm					
	L4	-.0007	1450	125	-.0014	7.5 (edge)
	L5	+.0198	50.5	38	.0386	7
	Plane Mirror: 50 x 70 mm					
CORRELATOR	Photocathode of PM: 2 inch Diameter					
	L6	+.0032	310	65	.0062	4
	L7	+.0072	140	70	.0140	9
	L8	+.0125	80	48	.0244	7.5
	Prism, Angle of Deviation = 15°					
COMMON TO VOS AND CORRELATOR	Beamsplitter Cube 40 x 40 mm; T(CORR): T(VOS) = 85:15					
	Aperture Diaphragm, A.D., Iris, Max. Dia. = 31 mm					
	L9	+.0097	103	37	.0189	3.5
	L10	+.0170	59	37	.0332	6
	L11	+.0170	59	30	.0333	30

*About 1/3 of this value has to be added for mechanical distance as compared to optical distance.

APPENDIX B

OBJECTIVE AND INTERMEDIATE LENSES

Tables B-1 and B-2 represent the first, tentative design approach. They are reprinted from Tables C1 and C2 of the second monthly report. After looking further into the requirements for the image rotator and for the zoom system it became clear that a distance between primary image and intermediate lens as determined by f_{int} = 450 mm is too small. Therefore, f_{int} = 540 mm has been chosen for design approach 2 (Table B-3).

A discussion with Contracting Office representatives revealed that it is desirable to expand the range of lens 2 so that a conventional work range between 40x and 90x can be covered without the necessity of switching lenses within this range of magnification. This is possible by increasing the zoom range from $m'_z = 1.0 \longrightarrow 1/3.0$ to $m'_z = 1.0 \longrightarrow 1/3.5$. The overlap between lenses 2 and 3, and also between lenses 1 and 2 is then considerably increased. In the attempt to realize this objective the focal length of the intermediate lens is kept at f_{int} = 540 mm and the diameter of the primary image at 2y' equals 18 mm (design approach 3, Table B-4). This approach requires an increase in magnification, $m'_{obj.}$ for lens Nos. 2 and 3, and a decrease in the respective F/numbers, or an increase in the corresponding numerical aperture NA. But this is the inevitable price which has to be paid for the increased magnification range. On the other hand, field angles for the first image will slightly decrease from $2\phi' = 6.90°$ to 6.65° for the full area and from $2\phi' = 2.30°$ to 1.91° for the center area (area of highest resolution).

The disadvantage of approach 3 is that the maximum diameter of the first image, that is before zooming, has to be 3.5 x 18 = 62.5 mm.

TABLE B-1

OPTICAL PARAMETERS FOR INPUT SIDE OF VISUAL OBSERVATION SYSTEM

Design Approach (1)

	1 $m'_{obj.}$ (Objective) Magnification Range	2 m'_Z (Zoom)	3 m'_C (Combined)	4 Object Field Diameter 2y [mm]	5 Object sp. Numer. Ap. NA = sinα	6 Resolution Required R[lines/mm]	7 Absolute Resolution; Lines Over Object Field	8 Prim. Image Numer. Ap. NA' = sinα'	9 Aperture Angle 2α' at Prim. Image	10 $f_{Obj.}$[mm] F/Number
1)	20x	1.0	20x	o.9	o.55	1000	900	o.0275	3.15°	22.5
	200 - 67	o.33	6.67	2.7	o.26	480	1290	o.0392	4.58°	F/o.9
2)	7.5x	1.0	7.5	2.4	o.288	525	1260	o.0385	4.40°	60
	75 - 25	o.33	2.5	7.2	o.104	190	1370	o.0420	4.80°	F/1.75
3)	3x	1.0	3x	6	o.121	220	1320	o.0403	4.60°	150
	30 - 10	o.33	1x	18	o.044	80	1440	o.0440	5.04°	F/4.1

Demagnifying Zoom - System 1⟶1/3; f_{int} = 450 mm; diameter of primary image 2y' = 18 mm.

TABLE B-2

LENS SPECIFICATIONS

Design Approach (1)

The field angle for the 'full" area is $2\vartheta = 6.88°$, for the 'center' area $2\vartheta = 2.30°$. Lens No. 4 refers to "intermediate lens'. Lenses No. 1-3 image into infinity; lens No. 4 from infinity. The aperture diaphragm of lenses 1 and 2 has to be in their back focal planes (telecentric lenses).

Lens No.	1 Assigned Magnification $m'_{Obj.}$	2 Focal Length $f_{obj.}$ [mm]	3 Numer. Ap. for Center Area NA = sinα	4 Corresponding F/number	5 Numer. Ap. NA for Full Field	6 Full Field Diam. 2y [mm]	7 Resolution for Full Field R[lines/mm]	8 Resolution in Center Area ~ R[lines/mm]	9 Diameter of Center Area [mm]	10 Diam. of Ap. Diaphragm [mm]
1	20x	22.5	o.55	o.9	o.265	2.7	480	1000	o.9	25
2	7.5x	60	o.288	1.75	o.104	7.2	190	525	2.4	34
3	3x	150	o.121	4.1	o.044	18	80	220	6	37
4		450	o.044	11.5	o.015	54	30	80	18	50*

Resolution refers to overall systems resolution with reference to object (film) plane for lenses No. 1 to 3, with reference to first image plane for lens No. 4. It has been calculated from the diffraction limit with a safety factor of 2.0.

* Free lens diameter

TABLE B-3

OPTICAL PARAMETERS FOR INPUT SIDE OF VISUAL OBSERVATION SYSTEM

Design Approach (2)

	1 $m'_{obj.}$ (Objective) Magnification Range	2 m'_Z (Zoom)	3 m'_C (Combined)	4 Object Field Diameter 2y [mm]	5 Object sp. Numer. Ap. NA = sinα	6 Resolution Required R [lines/mm]	7 Absolute Resolution: Lines Over Object Field	8 Prim. Image Numer. Ap. NA' = sinα'	9 Aperture Angle 2α' at Prim. Image	10 $f_{Obj.}$ [mm] F/Number
1)	20x	1.0	20x	o.9	o.55	1000	900	o.0275	3.15°	27.0
	200 - 67	o.33	6.67x	2.7	o.26	480	1290	o.0392	4.58°	F/o.9
2)	7.5x	1.0	7.5x	2.4	o.288	525	1260	o.0385	4.40°	72.0
	75 - 25	o.33	2.5x	7.2	o.104	190	1370	o.0420	4.80°	F/1.75
3)	3x	1.0	3.0x	6	o.121	220	1320	o.0403	4.60°	180
	30 - 10	o.33	1.0x	18	o.044	80	1440	o.0440	5.04°	F/4.1

Demagnifying Zoom - System 1⟶1/3; f_{int} = 540 mm; diameter of primary image 2y' = 18 mm.

TABLE B-4

OPTICAL PARAMETERS FOR INPUT SIDE OF VISUAL OBSERVATION SYSTEM

Design Approach (3)

	1 $m'_{obj.}$ (Objective) Magnification Range	2 m'_Z (Zoom)	3 m'_C (Combined)	4 Object Field Diameter 2y [mm]	5 Object sp. Numer. Ap. NA = sinα	6 Resolution Required R[lines/mm]	7 Absolute Resolution; Lines Over Object Field	8 Prim. Image Numer. Ap. NA' = sinα'	9 Aperture Angle 2α' at Prim. Image	10 $f_{Obj.}$ mm F/Number
1)	20x	1.0	20x	o.9	o.550	1000	900	o.0275	3.15	27.0
	200 - 57.5	o.288	5.75	3.13	o.229	415	1300	o.0400	4.58	F/o.9
2)	9x	1.0	9x	2.0	o.332	605	1210	o.0370	4.24	60
	90 - 25.9	o.288	2.59	6.95	o.110	200	1395	o.0425	4.87	F/1.5
3)	3.48	1.0	3.48	5.18	o.146	266	1380	o.0421	4.83	155
	34.8 - 10	o.288	1.0	18.0	o.044	80	1440	o.0440	5.04	F/3.4

Demagnifying zoom system 1⟶1/3.5

f_{int} = 540 mm

2y' = 18 mm

B-5

This would require an increase of the effective free aperture diameter of the K-mirror, resulting in an increase of the optical length through the K-mirror. It is very desirable to make the maximum free aperture of the K-mirror not larger than 55 mm, which would then keep the optical path through the K-mirror at about 300 mm. Therefore, an image diameter of $2y'_{Dr} = 15.5$ mm has been chosen in design approach 4 (Table B-5). In order to retain an image field diameter of $2y'_{OC} = 18$ mm at the ocular, the product of periscope magnification, m'_{Per}, (until now always assumed to be 1.0) and of ocular magnification, m'_{Oc}, has to be

$$m'_{Per} \times m'_{Oc} = 11.612x$$

which should not pose a difficulty. The maximum diameter of the first image remains then $2y_1'(max) = 54$ mm.

However, with an optical path of 300 mm for the K-mirror, only 240 mm remain for the beamsplitter, whose optical path equals t/n, ($\approx$ 36 mm), the zoom system (at least 200 mm desired), fine focusing with the intermediate lens (about 20 mm desired), and a reserve for mechanical design. Without the latter, 246 mm are required and only 240 mm are available. A change of $f_{int} = 540$ to $f_{int} = 600$ mm for the focal length of the intermediate lens would again result in a chain of difficulties, which can be avoided by the design approach 5. With the latter approach the input lens and K-mirror parameter remain the same, but a negative lens is placed between K-mirror and beamsplitter, bringing the magnification of the first image again up to 18 mm for the center field and 62.5 for the full field without the necessity of increasing the dimensions of the K-mirror. The optical path available for beamsplitter and zoom system is then increased, a diameter for the primary image of 18 mm is retained, which makes it possible to examine the primary image

TABLE B-5

OPTICAL PARAMETERS FOR INPUT SIDE OF VISUAL OBSERVATION SYSTEM

Design Approach (4)

	1 $m'_{Obj.}$ (Objective) Magnification Range	2 m'_Z (Zoom)	3 m'_C (Combined)	4 Object Field Diameter 2y' (mm)	5 Object sp. Numer. Ap. NA = sinα	6 Resolution Required r lines/mm	7 Absolute Resolution; Lines Over Object Field	8 Prim. Image Numer. Ap. NA' = sinα'	9 Aperture Angle 2α' at Prim. Image	10 $f_{Obj.}$ (mm) F/Number
1 a	18x	1.0	18.0	o.861	o.56	1020	875	o.0311	3.56	30
1 b	209 - 60	o.2870	5.167	3.000	o.237	431	1295	o.0459	5.24	F/o.896
2 a	7.714	1.0	7.714	2.009	o.327	595	1195	o.0390	4.46	70
2 b	89.5 - 25.6	o.2870	2.213	7.000	o.110	200	1395	o.0497	5.68	F/1.529
3 a	3x	1.0	3.00	5.167	o.146	265	1370	o.0487	5.56	180
3 b	34.8 - 10	o.2870	o.861	18.0	o.044	80	1440	o.0510	5.84	F/3.42

Demagnifying Zoom System 1⟶1/3.483;

f_{int} = 540 mm

2φ(min) = o.0287 = 1.645°; 2y'(min) = 15.5 mm

2φ(max) = o.100 = 5.72°; 2y'(max) = 54 mm

$m'_{Per} \times m'_{Oc}$ = 11.612 so that $2y'_{Oc}$ = 18 mm

with the eyepiece used for the observation station. Should, however, the increase of optical path not suffice, the possibility still exists of increasing the power of the negative lens. This would further lengthen the optical path, though the size of the first and the primary image will also increase (which would not pose a serious difficulty), without the necessity of changing the design parameter of condenser, objectives, and K-mirror. Thus, a higher design freedom is gained from this approach which is an important advantage. Leaving the diameter of the primary image, for the time being, at $2y'_{pr} = 18$ mm, the following will result:

Making the distance between intermediate lens and negative lens, t_1, equal 325 mm, the height of incidence, y_1, at the negative lens for the paraxial chief ray is (with $\bar{y}_2 = 27$ mm in the plane of the first image)

$$\bar{y}_1 = 27 \times 325/540 = 16.25 \text{ mm}$$

and slope angle of this ray in front of the negative lens:

$$\bar{u}_o = 27/540 = o.0500$$

The slope angle of the corresponding paraxial position ray is (in front of the negative lens) ($t_1 = 540 - 325 = 215$)

$$u_o = -\bar{y}_1/t_1 = -16.25/215$$

$$= -o.075,581$$

Resulting in the height, y_o, at the intermediate lens of (t = 540)

$$y_o = -u_o = o.075,581 \times 540$$

$$= 40.813 \text{ mm}.$$

The image diameter in image plane (2) shall be increased from 15.5 to 18.0. The slope angle behind the negative lens is then, because of the Helmholtz-Lagrange equation,

$$u_1 = u_o \times 15.5/18.0$$

$$= -o.065,083.$$

The required power, F_1, of the negative lens follows from

$$F_1 = -(u_1 - u_o)/\bar{y}_1$$

$$= -o.010,498/16.25$$

$$= -o.000,646$$

$$f_{neg} = 1548 \text{ mm}$$

and the distance, t_1, from negative lens to image plane increases from 215 mm to

$$t_1 = -\bar{y}_1/u_1$$

$$= 249 \text{ mm}$$

The combined focal length of both lenses is

$$f \text{ (int. + neg.)} = -y_o/u_1$$

$$= 627.091 \text{ mm}$$

Since the space requirement for fine focusing by means of the intermediate lens has been considered already (by assuming t_o = 325mm), this suffices for the zoom system (t = 200 mm) and the beamsplitter ($t_{opt} \approx$ 36 mm), leaving a reserve of 23 mm for the designer. The negative lens is not very strong and it may be used for the fine correction of some aberrations.

The advantages obtained justify the use of this negative lens. The overall results are shown in design approach 5, (Tables B-6 and B-7). The question may be brought up again at this time whether the safety factor of 2 in determining the NA or F/number of the objective lenses as required by resolution is a realistic one or is too overcautious (see eq. 4b, Appendix C2, of the second monthly report). It is planned to discuss this question in detail with the prospective subcontractor for the lens and periscope design.

It will, to a large extent, depend upon the proper balance between complexity of design (and price) on the one hand, and strict adherence to resolution specifications on the other hand. It should be kept in mind, however, that the question of numerical aperture - F/number also enters into the question of illumination. The exit pupil, EX, for diffraction limited visual instruments is about 1.0 mm, while EX $\simeq$ 2.0

TABLE B-6

OPTICAL PARAMETERS FOR INPUT SIDE OF VISUAL OBSERVATION SYSTEM
Design Approach (5)

	1 $m'_{Obj.}$ (Objective) Magnification Range	2 m'_z (Zoom)	3 m'_c (Combined)	4 Object Field Diameter 2y [mm]	5 Object sp. Numer. Ap. NA = sinα	6 Resolution Required R lines/mm	7 Absolute Resolution; Lines Over Object Field	8 Prim. Image Numer. Ap. NA' = sinα'	9 Aperture Angle 2α' at Prim. Image	10 $f_{Obj.}$ [mm] F/Number
1a	20.903	1.0	20.903	o.861	o.558	1016	875	o.0266	3.05	30
1b	209⟶60	o.2870	6.000	3.000	o.237	432	1295	o.0395	4.53	F/o.896
2a	8.958	1.0	8.958	2.009	o.327	595	1195	o.0365	4.18	70
2b	89.6⟶25.7	o.2870	2.570	7.000	o.110	200	1395	o.0428	4.91	F/1.529
3a	3.483	1.0	3.483	5.167	o.146	265	1370	o.0419	4.80	180
3b	34.8⟶10	o.2870	1.000	18.0	o.044	80	1440	o.0440	5.043	F/3.42

Demagnifying Zoom System m'_z = 1.0⟶1/3.483; intermediate plus negative lens f(int. + neg.) = 627.091 mm keeping light pencil diameter through K-mirror below 55 mm.

For the first image (before action of zoom system) 2y'(min) = 18 mm; 2y'(max) = 62.5 mm.

Table B-7

LENS SPECIFICATIONS

Design Approach (5)

The field angle for the "full" area is 2ϕ = o.100 rad = 5.731°, for the center area 2ϕ = o.0287 rad = 1.645°. Lens No. 4 refers to "intermediate lens", lens No. 5 to "negative lens" assumed to be 325 mm behind intermediate lens. Total optical distance from intermediate lens to first and primary image is then 574 mm or 249 mm optical path from negative lens to image with a glass path (beamsplitter quartz) of 58 mm; the equivalent optical path of 38.4 mm is included in the 249 mm quoted.

Lenses Nos. 1-3 image into infinity, lens No. 4 and No. 5 from infinity. The aperture diaphragm of lenses 1 and 2 has to be in their back focal planes (telecentric lenses).

Lens No.	1 Nominal Magnification $m'_{Obj.}$	2 Focal Length $f_{obj.}$ [mm]	3 Numer. Ap. for Center Area NA = sinα	4 Corresponding F/number	5 Numer. Ap. NA for Full Field	6 Full Field Diam. 2y [mm]	7 Resolution for Full Field R[lines/mm]	8 Resolution in Center Area R[lines/mm]	9 Diameter of Center Area [mm]	10 Diam. of Ap. Diaphragm [mm]
1	21x	30	o.558	o.90	o.237	3.0	432	1016	o.86	33.5
2	9x	70	o.327	1.53	o.110	7.0	200	595	2.0	46
3	3.5x	180	o.146	3.4	o.044	18.0	80	265	5.2	53
4	(interm.)	540	o.051	9.8	o.0146	54.0	32.6	93	15.5	50*
5	(negat.)	1548	o.044	11.4	o.0127	62.5	28	80	18.0	52*

Resolution (columns 7 and 8) refers to overall systems resolution with reference to object (film) plane for lenses No. 1 to 3, with reference to respective first image planes for lenses No. 4 and 5. Numerical apertures, NA (columns 3 and 5), refer to object space for lenses No. 1 to 3, to image space for lenses No. 4 and 5. They are obtained from the diffraction limit for the specified resolution with a safety factor of 2(NA = $R \cdot \bar{\lambda}$ = o.55 x R/1000).

* Free lens diameter

was assumed previously; therefore, the safety factor 2x appears in that context also. For the time being, further design considerations will be based on the results obtained by design approach 5, Tables B-6 and B-7. An attempt has been made to keep the focal lengths of the objectives at round numbers so that the possibility of using commercially available lenses is not blocked. (This explains why other numbers appearing in Tables B-6 and B-7 are not round numbers.)

In order to complete the discussion, two further approaches which were discarded have to be mentioned.

The first(design approach 6, Table B-8) serves to answer the question whether a de-magnifying zoom system ($m'_z = 1.0 \longrightarrow 1/3.5$) or a magnifying zoom system ($m'_z = 3.5 \longrightarrow 1.0$) should be chosen. (Design approach 6 is comparable to design approach 2, Table B-3). Design approach 6 requires, of course, objectives with a smaller, initial magnification, $m'_{Obj.}$, because an additional magnification will be obtained by the zoom system. The magnification of 6x, 3x, and 1x have been chosen tentatively for $m'_{Obj.}$, utilizing only $m'_z = 3.33 \longrightarrow 1.0$ for lenses Nos. 1 and 2. Since resolution requirements remain the same, the numerical aperture, NA, or the corresponding F/number, has to remain the same for each lens as on approach 2. The resulting lenses (column 10) are then very bulky, and, therefore, expensive. The fact that the maximum field angle will be reduced from $2\phi(max) = 6.85°$ (approach 2) to $2\phi(max) = 1.92°$ (approach 6) does not weigh very heavily, because

TABLE B-8

OPTICAL PARAMETERS FOR INPUT SIDE OF VISUAL OBSERVATION SYSTEM

Design Approach (6)

	1 $m'_{Obj.}$ (Objective) Magnification Range	2 m'_z (Zoom)	3 m'_C (Combined)	4 Object Field Diameter 2y [mm]	5 Object sp. Numer. Ap. NA = sinσ	6 Resolution Required R[lines/mm]	7 Absolute Resolution; Lines Over Object Field	8 Prim. Image Numer. Ap. NA' = sinσ'	9 Aperture Angle 2σ' at Prim. Image	10 $f_{Obj.}$ [mm] F/Number
1)	6x	3.33	20x	o.9	o.55	1000	900	o.0275	1.65	90
	200 - 60	1.0	6x	3.0	o.238	431	1295	o.0396	2.26	F/o.9
2)	3x	3.33	10x	1.8	o.360	655	1180	o.0360	2.06	180
	100 - 30	1.0	3x	6.0	o.1265	230	1380	o.0422	2.42	F/1.4
3)	1x	3.5	3.5x	5.14	o.1463	266	1365	o.0418	2.39	540
	35 - 10	1.0	1x	18.0	o.044	80	1440	o.044	2.52	F/3.4

Magnifying Zoom System $m'_z = 3.5 \longrightarrow 1.0$

$2y' = 18$ mm diameter of primary image

$f_{int} = 540$ mm

this decrease of field angle does not appreciably help the lens designer, as compared to the difficulties he encounters in designing an F/0.9 lens with a field of about 7 degrees and a focal length of about 25 mm (wavelength will be the same in both cases but lens diameters will change). Another negative aspect of this approach is the fact that the 1x objective with a focal length of $f_{Obj.}$ = 540 mm has to be integrated into the system. This will obviously make the system much bulkier. These are reasons enough to drop this design approach.

Design approach 7, Table 9 will serve to illustrate the possibilities of a system with only one objective lens, but a zoom system with which the entire range of m'_x = 1.0 1/20 can be covered. In order to be comparable to design approach 2, this approach is based on the same optical parameters as approach 2, in particular a focal length $f_{Obj.}$ = 27 mm and a diameter for the primary image 2y' = 18 mm.

Table 9 shows that the objective lens has to cover an extremely large range, namely, a change of field from

$$2y = 0.9 \longrightarrow 18.0 \text{ mm}$$

or a corresponding field angle of

$$2\phi = 1.84° \longrightarrow 36.8°$$

while the numerical aperture changes from

$$NA = 0.55 \longrightarrow 0.044$$

or the corresponding F/number from

$$F = 0.9 \longrightarrow 11.4.$$

It is very doubtful that the design of such a lens is possible in view of the high resolution requirements, or even that it would be practical if the contracting agency is lenient with respect to complete fulfillment of resolution requirements. Reasons for this doubt are found in the fact, which is well known to experienced

TABLE B-9

OPTICAL PARAMETERS FOR INPUT SIDE OF VISUAL OBSERVATION SYSTEM

Design Approach (7)

	1 $m'_{Obj.}$ (Objective) Magnification Range	2 m'_z (Zoom)	3 m'_c (Combined)	4 Object Field Diameter 2y [mm]	5 Object sp. Numer. Ap. NA = sinα	6 Resolution Required R[lines/mm]	7 Absolute Resolution; Lines Over Object Field	8 Prim. Image Numer. Ap. NA' = sinα'	9 Aperture Angle 2α' at Prim. Image	10 $f_{Obj.}$ [mm] F/Number
	20x	1.0	20x	o.9	o.55	1000	900	o.0275	3.15°	27.0
	200 - 10	1/20	1x	18	o.044	80	1440	o.044	5.04°	F/o.9

Demagnifying Zoom System with m'_z = 1.0⟶1/20 diameter of primary image 2y' = 18 mm

lens designers, that requirements for small field and large numerical aperture run counter to the requirements for large field and small numerical aperture. Of course, certainty about this point can be obtained only by actually working on the design of a lens of this kind and seeing what results can be obtained from a methodical and diligent study. However, it is felt that such an approach deviates so much from established practice and proven experience that the effort should not be undertaken.

There are other points raising doubts in connection with approach 7. If a one-step zoom system is used, it will again be difficult to design it (optically) so that it will in no position impair image quality. Usually, zoom lenses are farther from the diffraction limit than conventional, non-zooming photographic lenses. It is very difficult to minimize aberrations, so that they are negligible, in an optical system where the position of the lenses changes. The difficulties become greater as the position changes, i.e., the zoom ratio, becomes larger. Also, the large maximum field angle which now appears makes it advisable to place the zoom lens as close to the objective lens as possible, otherwise the optical cross section will become impractically large. But then, other system components cannot be placed as near to the objective lens as is found desirable, in order to make them insensitive to changes in the optical train, such as the beamsplitter to bring in the floating dot, beamsplitter for the correlation, and the image rotator.

A two-step zoom system could be considered, the first step behind the objective lens, the second step combined with the observation station, namely, the ocular. But if the zoom-system, or part of it, is integrated with the ocular, the anamorphic eyepiece cannot be placed in the ocular any more.

There are other difficulties involved with either a one-step 1:20 zoom system or a two-step zoom system each 1:4.5. Even if these difficulties do not make an approach of this kind absolutely impossible, they will certainly require compromises with other design details, which are just as important for the overall system design and its performance.

This discussion leaves design approach 5 (Tables B-6 and B-7) as the one with the highest promise for a good hardware design. Figure B-1 outlines the arrangement of optical parts for the "input station". A small compromise was found desirable; the free diameter of the intermediate lens was held at 50 mm and that of the negative lens at 52 mm as compared to a full field diameter of 53 mm for the 3.5x objective. This compromise is necessary to keep the required optical path through the K-mirror short, but does not seriously impair optical performance in view of the safety factor of 2.0 in calculating the required aperture. The beamsplitter cube has been increased to 58 mm (38.4 mm optical path) to insure good performance.

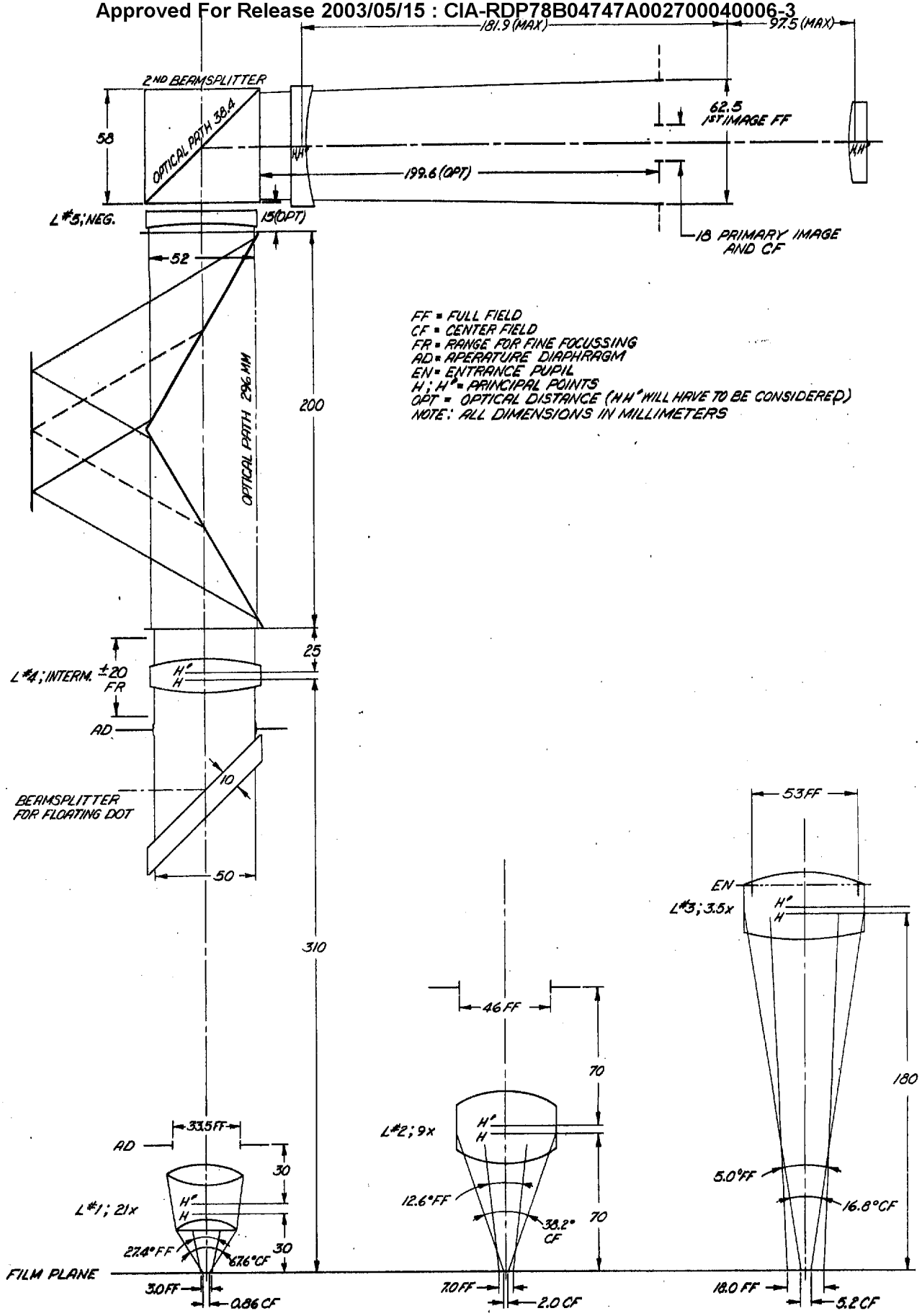

VISUAL OBSERVATION SYSTEM INPUT STATION

FIGURE B-1

RETICLE DOT SUBSYSTEM

C 1. General Arrangement and Design Considerations

It is necessary that the floating, or reticle, dot, F.D., be placed as close to the objective lens of the input station as possible. Insertion of any additional optical elements between these components carries the danger of influencing the position of the reference dot by movements of either the frame to which the element is mounted (because of temperature effects or changing loads) or, if the optical element is not rigid, by undesirable but unavoidable imperfections in its moving mechanism.

The latter applies particularly to the zoom system. It does require optical elements moving along the optical axis (i.e., longitudinally), and a reasonable tolerance for lateral movement accompanying the necessary longitudinal movement must be established because of imperfections in the track and moving mechanism. If the floating dot is brought into the optical train before it enters the zoom system the floating dot will participate in the resulting movements of the image thus serving as a reference fixed relative to the image.

This is the main reason for insertion of the floating dot immediately behind the objective lens, into the parallel light bundle between objective lens and the intermediate lens (see Optical Layout, Appendix B). The inevitable price which has to be paid for this approach is that the size of the floating dot has to change not only by the specification ratio of 1:8 (between 0.5 and 4.0 min of arc) but also by the zoom magnification ratio of 1:3.5. The total variation in reticle dot size therefore must be 28:1.

In theory it would be possible to reflect the floating dot through the objective lens upon the film, utilizing the scattering power

of the film emulsion to bring the floating dot image back through the objective lens into the observation station. However, this idea has been discarded. A strong argument against it is the fact that the floating dot image would then depend too much upon the scattering capability of the film, which varies considerably with film density (size and number of grains in the emulsion). The floating dot would be almost invisible in clear areas of the film where a high dot intensity is required because of the high background brightness in the film. Also, this approach does nothing to prevent motion of the floating dot relative to the film if the frame to which the floating dot mechanism is attached is not rigid. The relative movement of the floating dot because of an insufficient rigidity of its frame will be exactly the same if the floating dot is reflected directly into the optical train (without the detour over the film) as indicated in the Optical Layout.

The best protection against such dot movements is to mount the floating dot mechanism into the most rigid part of the instrument available for this purpose, that is the yoke carrying the "input station" and holding it in place over the film table. This approach does not guarantee absolute freedom from a relative motion between floating dot and the image of the film area; it only minimizes this danger. Extreme care will be needed in the mechanical design to hold the structure within the required tolerance.

There are several approaches possible for changing the apparent size of the floating dot image. The idea of using an optical zoom system like that for the VOS has been discarded for two reasons. First, the required zoom ratio of 1:28 is too large to be practical. Second, use of zoom lenses would make the instrument sensitive to possible inaccuracies of the track on which these lenses have to move. Because the floating dot should be used as a reliable primary reference point, it was considered to be better if this source

of possible error is avoided. This leads to the selection of a rigid optical system.

The optical system proposed will consist of a high quality telescope objective T.O. (see Figure C-1) of (at least approximately) the same focal length as the intermediate plus negative lens system in the VOS. Its distance from the floating dot beamsplitter, F.D.BS., is variable within a comparatively large range, because it images the floating dot, F.D., into infinity. Thus, the light between T.O. and beamsplitter is "parallel", in agreement with the general design concept. A 90 degree double mirror, M_1, M_2, folds the rays back toward the main tube. The floating dot, F.D., is formed in the focal plane of T.O. It is the demagnified image of a diaphragm, Dph., the nature of which will be discussed later. The demagnification is obtained by a commercially available microscope objective, M.O., a so-called apochromat corrected for use without cover glass and a so-called negative ocular or projector, Pr. The latter is used for highest quality micro-photography.

STAT

The diaphragm will be illuminated by a lamp, L.S., such as a "Concentrated Arc" lamp [redacted] or a Zircon-arc lamp, and a condenser, Cond. The condenser is divided into two parts with parallel light between them. A gray wedge, G.W., and if necessary, additional gray filters are placed in this area for a wide and continuous variation of the "intensity", or better luminance, of the floating dot image. The gray wedge requires, of course, a small fixed counter wedge with equal wedge constant in order to equalize this light distribution over the pupil area. The nature of this gray wedge will be discussed later.

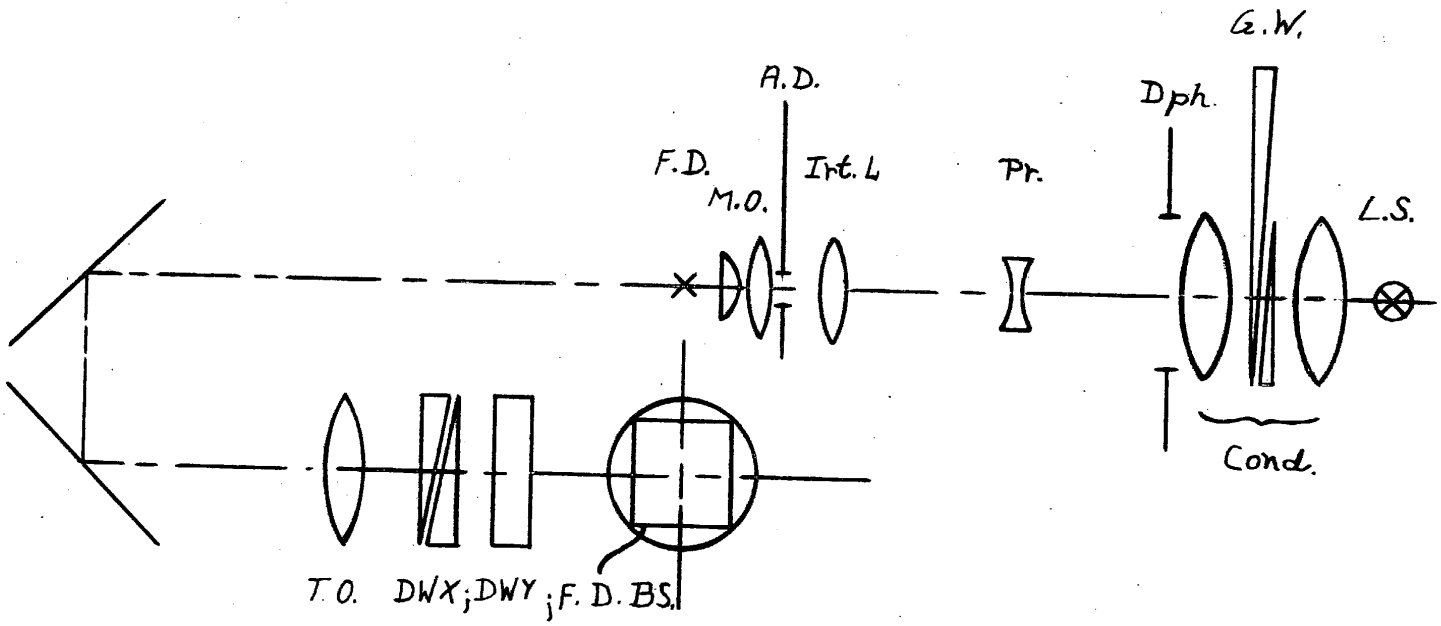

RETICLE DOT OPTICAL SYSTEM

Figure C-1

The exact adjustment of the floating dot in X (parallel to the eye base line) and Y (perpendicular to the eye base line) is very important and critical. If the two dots of both optical branches differ only little in Y, the observer is unable to fuse these two dots into one dot conceived as floating in space. A difference in X determines the parallax between the two dots, which is equivalent to the apparent distance of the floating dot in the three dimensional picture, or its Z coordinate. Because of the importance of this adjustment, it should have easy access and should be easy to handle in order to check and readjust the floating dot position whenever it is deemed necessary. It might even be advantageous to attach a measuring scale to the adjustment device in order to be able to compare several adjustments and to reset a previous adjustment.

It will be shown below that a very large demagnification will be applied to the diaphragm in order to assure high quality in the image. This demagnification relaxes the accuracy requirement for X and Y positioning of the diaphragm and conventional mechanical design techniques should suffice. However, because there will be a need for a mechanism to change the size of the diaphragm, it may be found desirable in the mechanical analysis to separate these three adjustments.

If this is found to be the case, it is possible to provide an optical adjustment which is sensitive and precise and located in the space between T.O. and the beamsplitter. The best means for an adjustment of this kind would be a rotating double wedge, DW, one for the X- and one for the Y-direction, DWX and DWY.

A double wedge consists of two prisms with a small prism angle mounted so that they can be rotated in opposite directions. In the zero-position, the two wedges supplement each other to form a plane parallel plate, which has no effect upon the quality of the dot image since it is placed where the light rays are parallel. In the position of maximum deviation, the two prisms supplement each other to form a prism with an angle twice the angle of one prism and a corresponding maximum deviation. This double wedge is a sensitive and precise device for measuring, or adjusting, small angle deviations, which became popular for the first time through its application in the range-finder of [redacted] cameras. STAT

It would, of course, be necessary to achromatize these prisms, but this is not a serious problem. It would theoretically suffice to have only one double wedge and to rotate the two prisms either counter (to determine the angle of deviation) or together (to move the point on a circle), but this is discouraged. A separate adjustment in X and Y without cross-talk between them seems a much better solution for this purpose. Therefore, use of a separate double wedge for each of the two adjustments is anticipated.

If the X-adjustment is provided with a remote control from the place of the operator and with a remote readout, it could be used to measure the difference in Z between two (spatial) image points in the observation station. It is probable that higher measurement accuracy for the difference of the X, Y, and Z coordinates of two points could be obtained by the double wedges than by table motion, provided the two points are visible within the field of view so that they can be measured with fixed table positions. This would make it possible to determine the dimensions of certain details (buildings, vehicles, etc.) with a higher accuracy than points of larger separation.

This method could be further improved by splitting the floating dot into two dots, one with only small adjustments in the center of the field, the other one with free movements throughout the field of, say, the 9x objective. This optional device will be called "Optical Stereo-Micrometer". (If time permits, a quantitative analysis will be given later.)

To implement this idea, the space between T.O. and F.D.BS. is again utilized. The light path is split into two branches (see Figure C-2) by a mirror arrangement similar to that used in [redacted] STAT interferometers. (This deviates from the details given in [redacted] STAT the proposal; but the approach here is much better.) Each branch is then equipped with two double wedges, in one branch with only small deviation angles for the center spot, in the other branch with larger deviation angles for the dot moving in the field of view. This device could be used by placing the center dot, say, on the top of a vehicle, and the other dot on its eight corners. In this way the dimensions of the vehicle might be obtained independently of, and with a higher accuracy, than with the metering system of two tables moving relative to one fixed floating dot.

C 2. RETICLE DOT OPTICAL ANALYSIS

If the focal length of T.O. is assumed to be f = 600 mm, a disc of one minute of arc viewing angle has a diameter of

$$600 \times 0.003 = 0.18 \text{ mm}$$

However, this will be magnified by the ocular in the observation station, which is assumed to have a magnification $m'_{Oc} = 10x$. So the value above corresponds to 10 minutes of arc. The range has to cover angular values of 0.5 to 14 minutes of arc because of the possible demagnification of 3.5x in the zoom system or for the F.D. diameter:

$$d'(\text{F.D.}) = 0.009 \longrightarrow 0.252 \text{ mm}$$

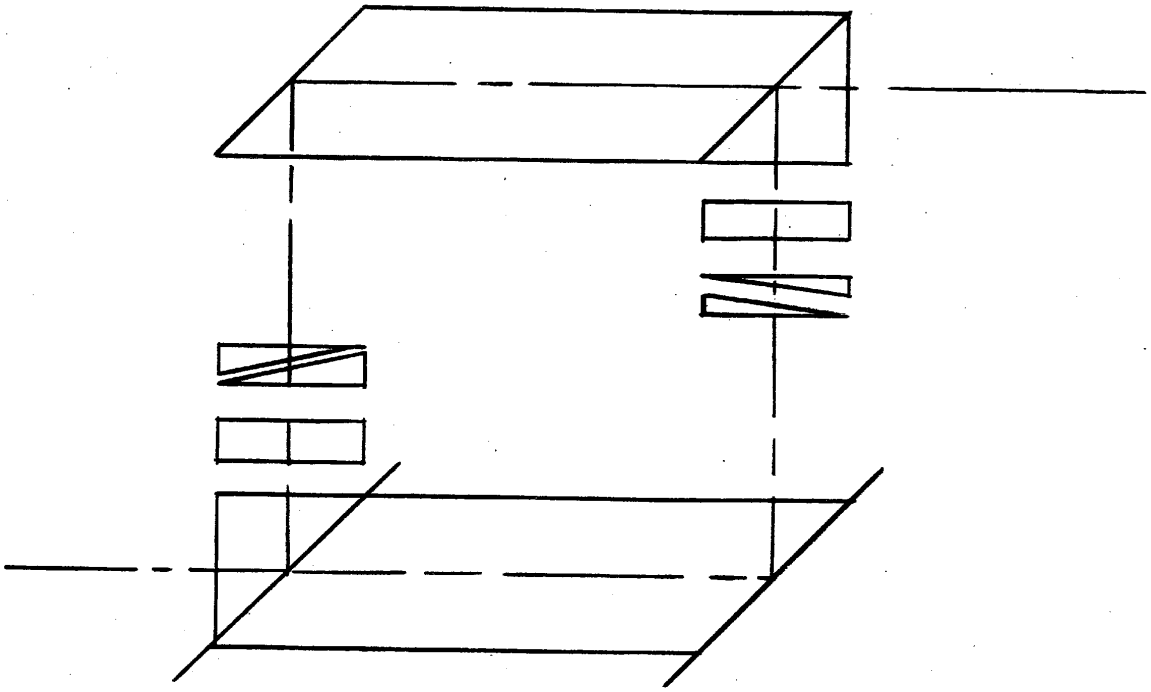

OPTICAL STEREO-MICROMETER

Figure C-2

which has to be obtained through demagnification by the microscope system mentioned above from a conveniently larger diaphragm.

It has been specified that the dot has to be a perfect circle at all times with a sharp edge gradient. It has to be kept in mind, however, that the dot is so small that inevitably diffraction effects will come into play. The angular diameter, δ, of the first minimum of an [redacted] disc follows from STAT

$$f_{oc} \cdot \delta = 2.44 \times \lambda/NA$$

where NA = numerical aperture in the image plane of the ocular. Assuming NA = 0.044, f_{oc} = 25 mm (m'_{oc} = 10x), and $\lambda = 0.55 \times 10^{-3}$ mm

$$\delta = 6.1 \times 10^{-4} [\text{rad}] = 2.1 \text{ min. of arc.}$$

If NA becomes smaller, δ will be correspondingly larger. If, however, the influence of aberrations is comparable to diffraction effects, first the light distribution in the [redacted] disc will change, STAT then, as the influence of aberrations increases, the Airy disc will be smeared out more and more.

If the stop which serves to produce the F.D. by demagnification corresponds to just about the size of an Airy disc, small deviations from perfect roundness such as those resulting from the lamellas of an iris will not be visible. The deviations from roundness will not be resolved by the eye on account of geometrical optical principles if irregularities are negligibly small as compared to the equivalent of one minute of arc. Diffraction effects are also negligible since the diffraction pattern of a many sided polygon approaches that of a round disc. (See, for instance, Born-Wolf; Principles of Optics, Section 8.5.2, footnote at the end of the first paragraph.)

This was tested experimentally, found true, and can be demonstrated. Also note: a starlike diffraction pattern is obtained not by small deviations of the fieldstop from roundness, but if the aperture diaphragm in the imaging lens is a distinct polygon (such as a triangle or square).

Since the dot is perceived stereoscopically, its position accuracy should be compatible with the depth or parallax resolution of the human eye, which is about ten times as good as the acuity of the eye (one minute of arc under optimum seeing conditions). The position accuracy should, therefore, be better than one-tenth of the equivalent diameter for one minute of arc.

If we assume that an iris diaphragm is acceptable, a precision diaphragm of not too small a diameter, manufactured by a well reputed firm, should be chosen: say a diaphragm between

$$d\ (Dph) = 2.5 \text{——} 70 \text{ mm},$$

so that the diameter corresponding to one minute of arc is 5.0 mm. The centering accuracy would then have to be = 0.5 mm or better. This seems attainable, though it might require careful laboratory checks of the products of several manufacturers.

The microscope demagnification required for these dimensions is

$$m'\ (micr) = 2.5/.009 = 278x$$

with an apochromatic objective of N.A. = 0.30 and m' = 12.5x STAT
[redacted] for instance), a magnification of 22x remains for the projector. Since apochromats corrected for use without cover glass are mostly those designed for metallographic microscopes which, in most cases, are infinity objectives in combination with an intermediate lens system, it will be wise to anticipate use of this kind of microscope optics. This makes it possible to restrict the N.A. to the required value of N.A. = 50/600 = 0.0835 by placing

an aperture diaphragm between objective and intermediate lens (as close to the objective as feasible). This aperture diaphragm has to be perfectly round and well centered.

OPTICAL CORRELATION

D 1. Theory of Operation

The operating principle of the Optical Correlator is illustrated in its simplest form in Figure D-1 . In this figure two transparencies, separated by an arbitrary distance, are placed along a common optical axis in front of a diffuse light source. An infinite number of bundles of parallel rays emerge from the light source and penetrate the two transparencies. If a lens is placed as shown, each of the parallel bundles of rays is brought to a focus in a plane, called the detection plane, located at the focal length of the lens.

Because of density variations in the transparencies there will be a distribution of light and dark areas in the detection plane. If an extreme example is taken, in which one transparency is a negative of the other, and if the photography is of such high contrast that transmission is limited to either zero or 100 per cent, then it can be recognized intuitively that there will be one particular bundle of parallel rays which will be blocked either at transparency #1 or transparency #2, and therefore there will be one point in the detection plane which will be completely black. This is the correlation peak, and its location with respect to the optical axis gives the X and Y displacement of the transparencies relative to each other. This location can be detected by an appropriate sensor. The above example is illustrative of a "quotient match". If the transparencies were identical copies, rather than a positive and negative, the correlation peak would consist of a bright spot, and this would be called a "product match".

In cases of practical interest the transmissions are not restricted to zero or 100 per cent, and for stereo pairs the imagery is not identical. While the principle of operation remains the same, these factors combine to reduce the contrast of the correlation peak with respect to the background. That is, the signal-to-noise ratio is degraded from that in the idealized case.

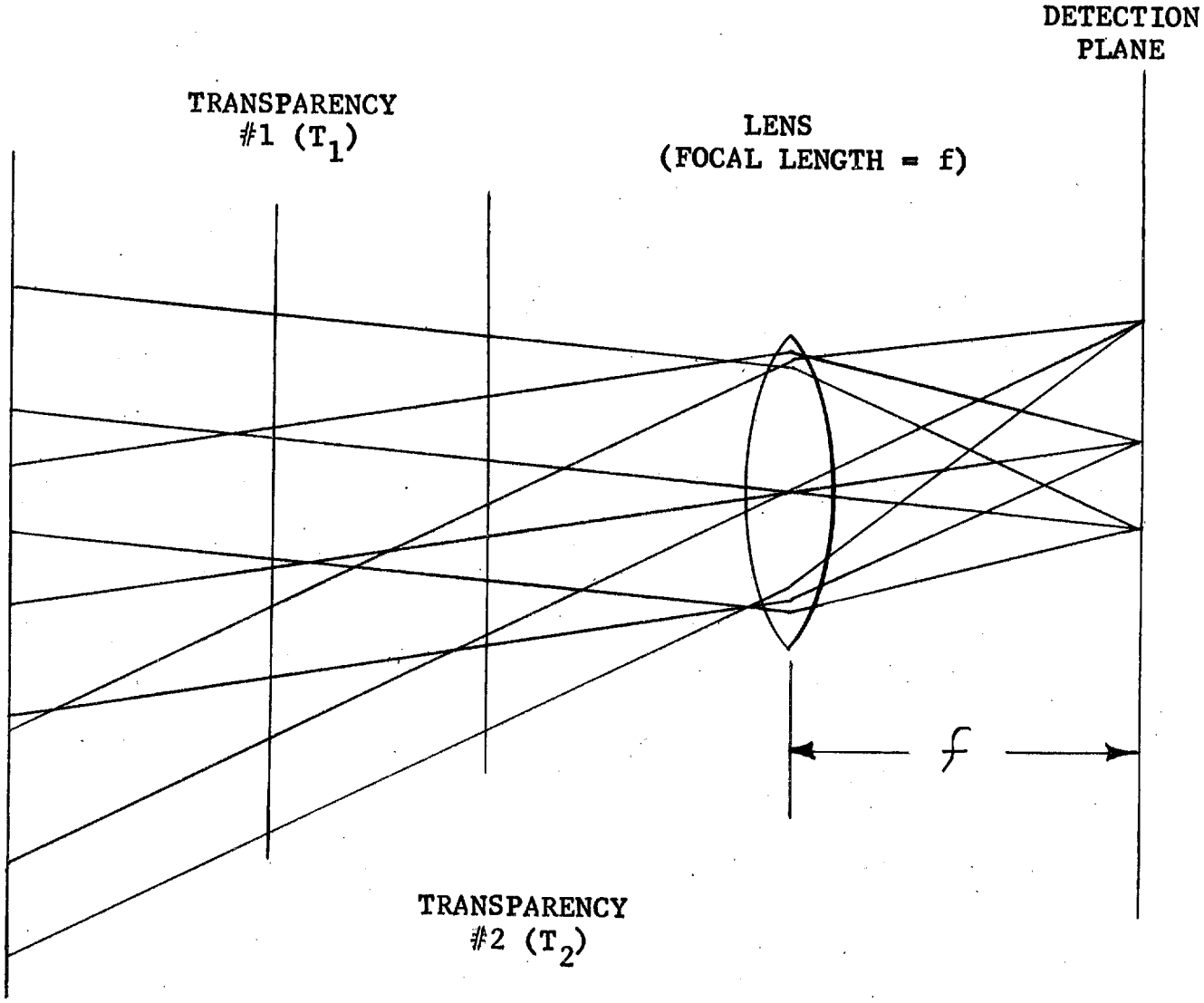

NOTE: Diagram assumes equal scale for T_1, T_2. Parallel rays which penetrate corresponding points of T_1, T_2 will produce the most prominent point in the detection plane. If T_2 is smaller scale than T_1, the rays of interest will be convergent, and the detection plane will therefore translate with respect to the lens.

BASIC CORRELATOR CONFIGURATION

FIGURE D-1

In practical cases it is found that any slight rotation of one field relative to the other from the exact registry position will cause the spot to disappear. A means of improving signal-to-noise ratio takes advantage of this phenomenon. One transparency can be rotated slightly relative to the other periodically to cause the spot to pulsate, and this variation can then be picked out of the relatively constant (DC) background by synchronous phase detection. This process is called dithering and can be accomplished either mechanically or electronically.

The photo position sensor chosen [redacted] STAT
[redacted] STAT
[redacted] This device was developed as a star tracker STAT
and will indicate the relative position of a spot of light (or darkness) on the photocathode.

D 2. Laboratory Models Implemented

The first working optical correlator implemented is a simple transparency-to-transparency matcher. This device is sketched in Figure D-2 and presented in the photograph of Figure D-3. Both fields are presented on film transparencies and illuminated by a diffuse incandescent light source. The lens focuses the correlation spot and immediately surrounding field onto a photo sensor cathode. The photo sensor employed [redacted] STAT
[redacted] The upper transparency is STAT
mounted on a X, Y, and Θ Transit Table. All table drives are manual. Dither was introduced for data taking purposes by rotating the top field (in the Θ sense) about 5 degrees. This was enough to make the spot disperse both to the eye and [redacted] The out- STAT
puts [redacted] were fed into [redacted] microvolt- STAT
meters. Readout was from these meters in microvolts. X and Y STAT
movements required to generate good match curves seldom exceeded

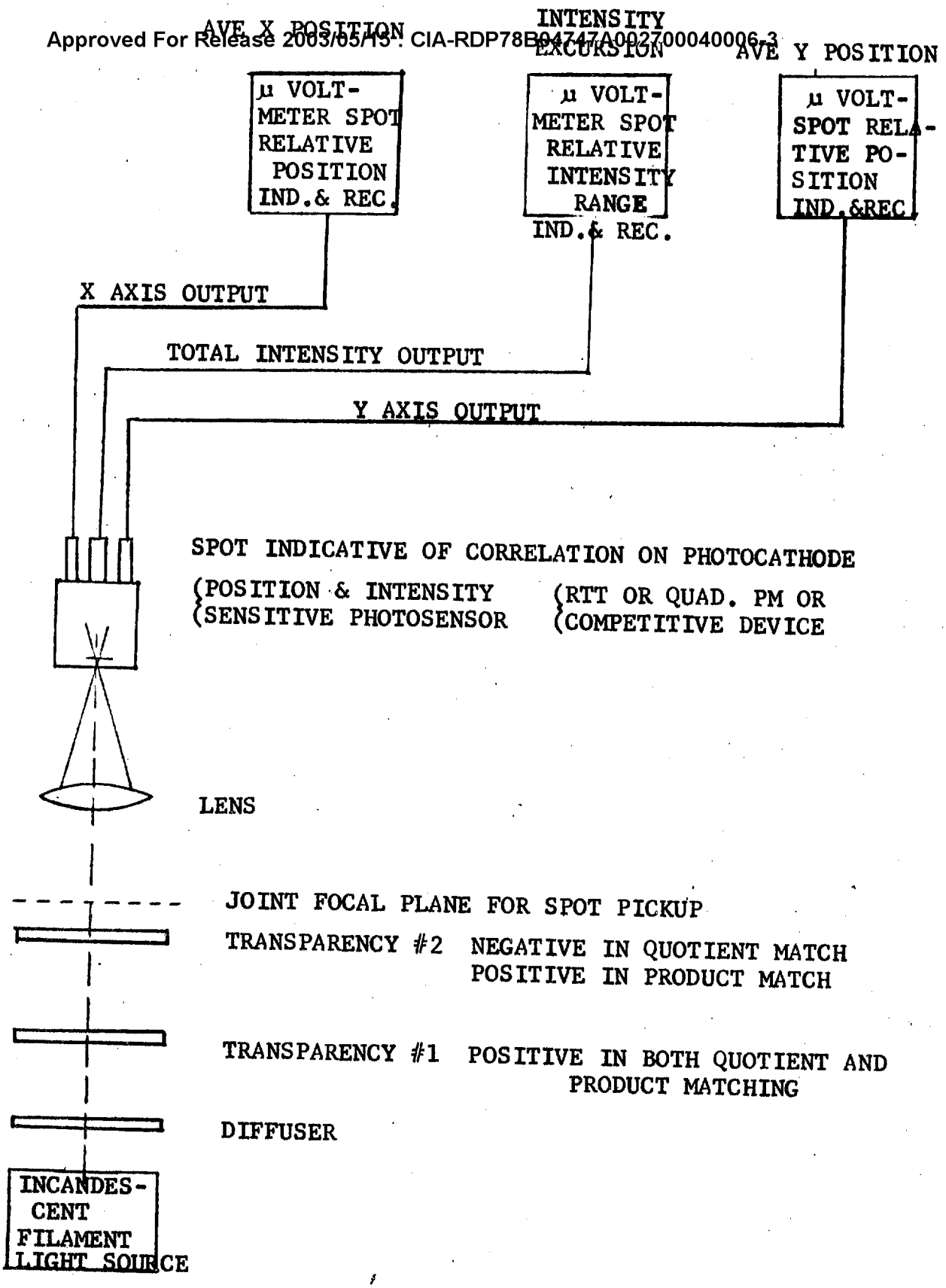

OPTICAL CORRELATOR SCHEME: TRANSPARENCY VERSUS TRANSPARENCY

FIGURE D-2

STAT

± 1.5 mm. [ ] response to this system is good. This is due to the fact that the [ ] natural spectral response is very similar to the emission spectra of incandescent (2900°K) tungsten. STAT STAT

In order to get a configuration applicable to the Stereo Comparator, a CRT-to-transparency matcher was implemented next. Figure D-4 presents the general idea, Figure D-5 presents a combination block and assembly diagram, and Figure D-6 is a photograph of the equipment.

This device functions so as to compare like fields of information but at different sizes or scales. The first transparency is scanned by a flying spot scanner and its imagery is presented in the face of the CRT. The imagery on film transparency to be correlated is of smaller size (i.e., scaled down) and is placed some experimentally determined distance away in register on the optical axis. The region near the apex of the pyramid developed will contain the spot. The viewer screen [ ] is placed in this region. STAT

The #2 transparency (on 35 mm film) was held on a transit table having X, Y, and Θ movement capability. Dither can be introduced either mechanically (via Θ mode of table) or electronically (pulsed X and Y deflection voltages). The [ ] outputs are fed into [ ] microvoltmeters for readouts. Table movements seldom exceed ± 1.5 mm for good match data generation. That is, lock-on for correlation is about ± 1.5 mm from true correlation point. Rotation required for effective spot dispersion (for dither) is about 5 degrees. STAT STAT STAT

[ ] response to the best of CRT phosphors [ ] slow) for this purpose is not good as compared to incandescent tungsten illumination. Everything else being constant, the illumination level of the [ ] display must be about fifty times that of the incandescent tungsten diffused source in order to produce the same signal out STAT STAT STAT

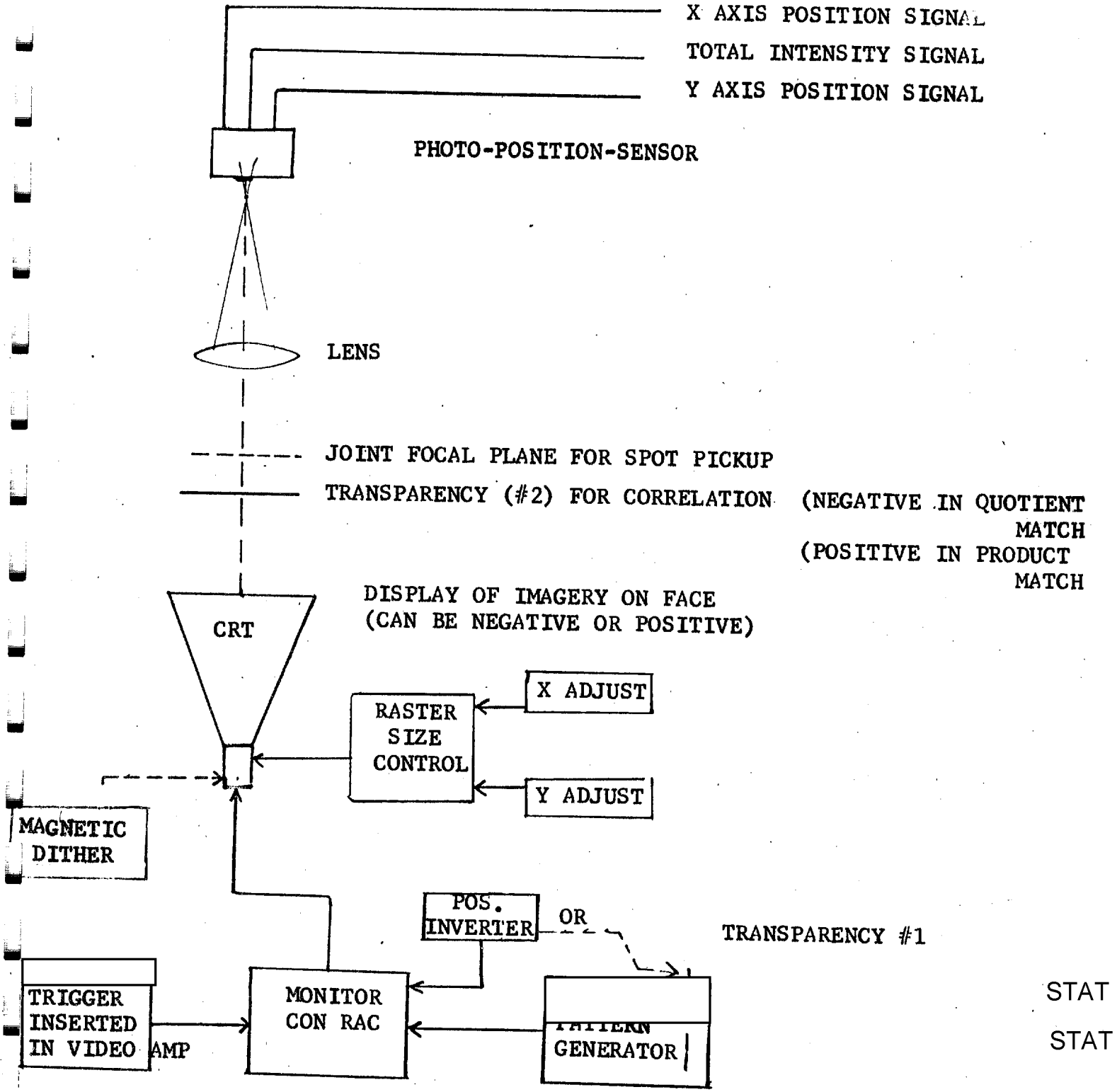

OPTICAL CORRELATOR SCHEME: CRT TO TRANSPARENCY

FIGURE D-4

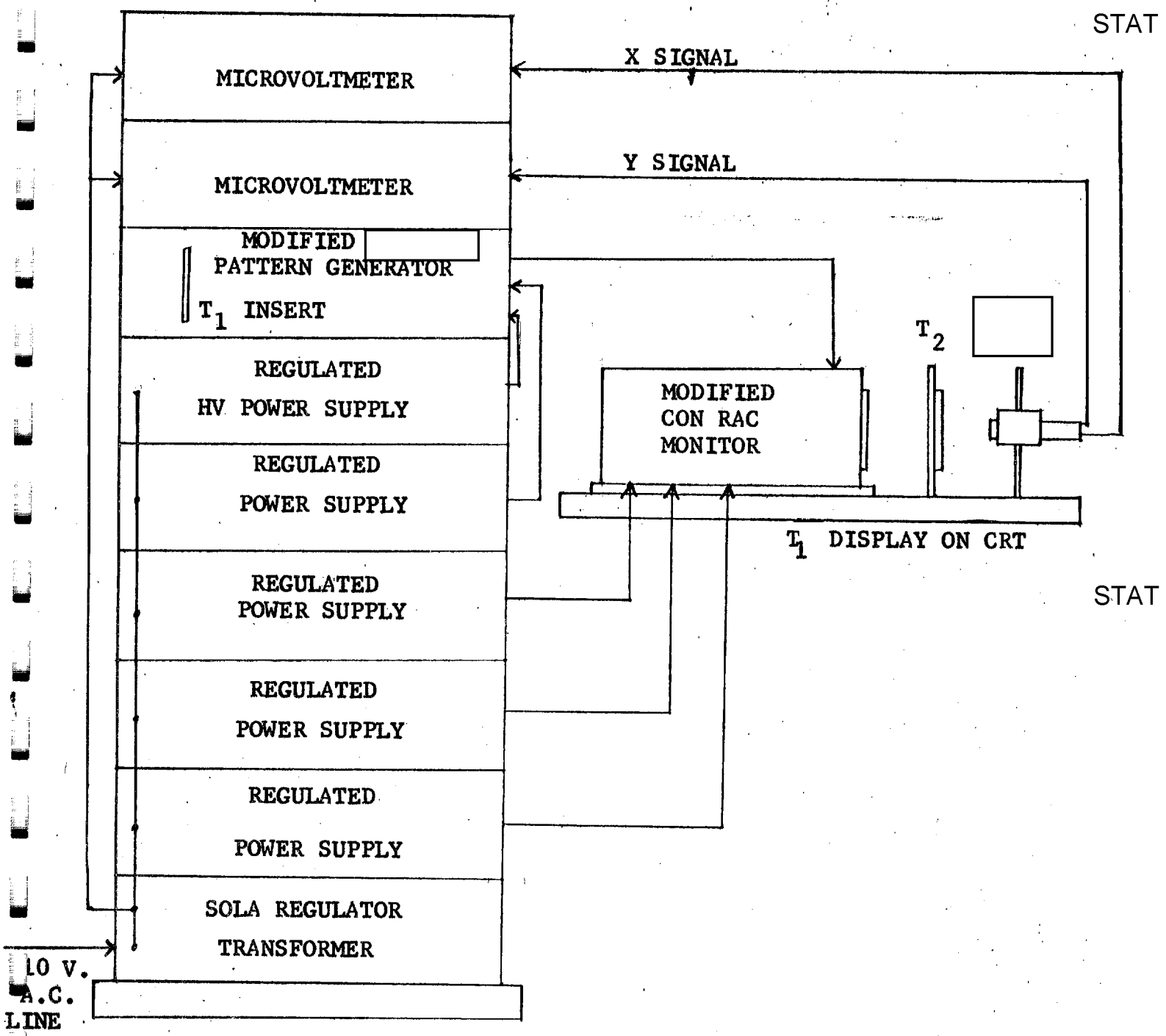

EQUIPMENT ASSEMBLY, FIRST CRT TO TRANSPARENCY CORRELATOR

FIGURE D-5

STAT

[redacted] In view of this fact, an image intensifier tube and STAT
associated power supplies would be required for working with small imagery and high density films. Figure D-7 is an assembly drawing which suggests how this might be implemented.

An improved, more versatile version of the CRT-to-transparency type Optical Correlator is presently being completed. It provides: (a) variable raster size, (b) automatic variable frequency electronic dithering, (c) small area vernier scanning (manually programmed), (d) a choice of scanning techniques (i.e., standard television, lissajous, triangular, random, etc.), (e) variable frame rate, (f) automatic dither demodulation and readout, (g) contrast and edge enhancement, (h) precision picture stability circuitry. It is illustrated in Figures D-8, D-9 and D-10.

D 3. Performance and Data

The performance of the optical correlators was largely dependent upon the response [redacted] to the spots generated. This appears STAT
to be a function of the illumination source emission spectrum. It was found that a blue or green peak sensitivity range [redacted] was not STAT
available. The present near IR peak (8400°) is the best available, giving excellent response to incandescent tungsten illumination. STAT
The phosphor best matching [redacted] (in the emission spectra versus STAT
spectral response sense) is the slow [redacted] This is also the best in the
the fact that very high brightness is easily obtainable from the
[redacted] STAT

The first data was taken using the transparency versus transparency apparatus of Figures D-2 and D-3 . Sample data from this apparatus is presented as Figure D-11. This is a presentation of a series of match curves about the true match point. The imagery was synthetic (random checker pattern) on [redacted] (second generation) STAT
type film. The imagery was illuminated by diffuse incandescent tungsten (2900°K) light. A positive transparency was compared with

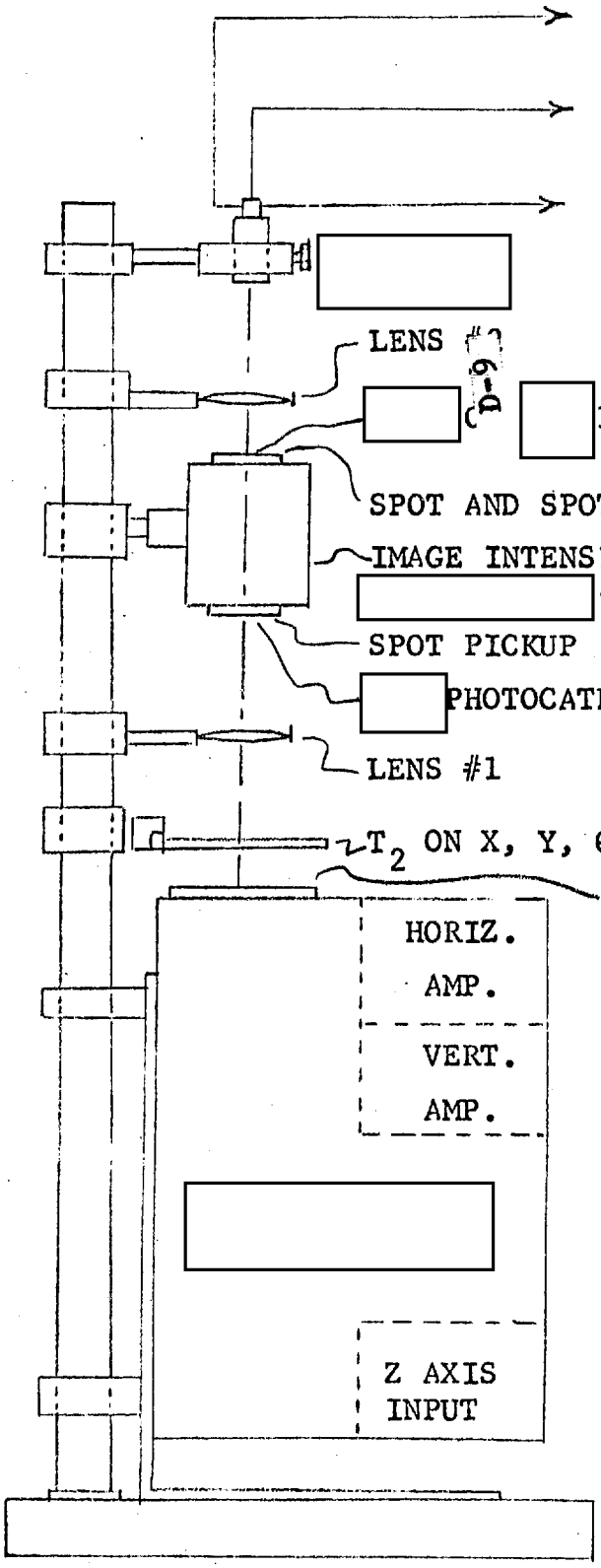

STAT STAT STAT STAT STAT STAT

OPTICAL CORRELATOR CRT VS. TRANSPARENCY WITH IMAGE INTENSIFIER

FIGURE D-7

STAT

Next 1 Page(s) In Document Exempt

Approved For Release 2003/05/15 : CIA-RDP78B04747A002700040006-3

STAT STAT

STAT STAT

STAT

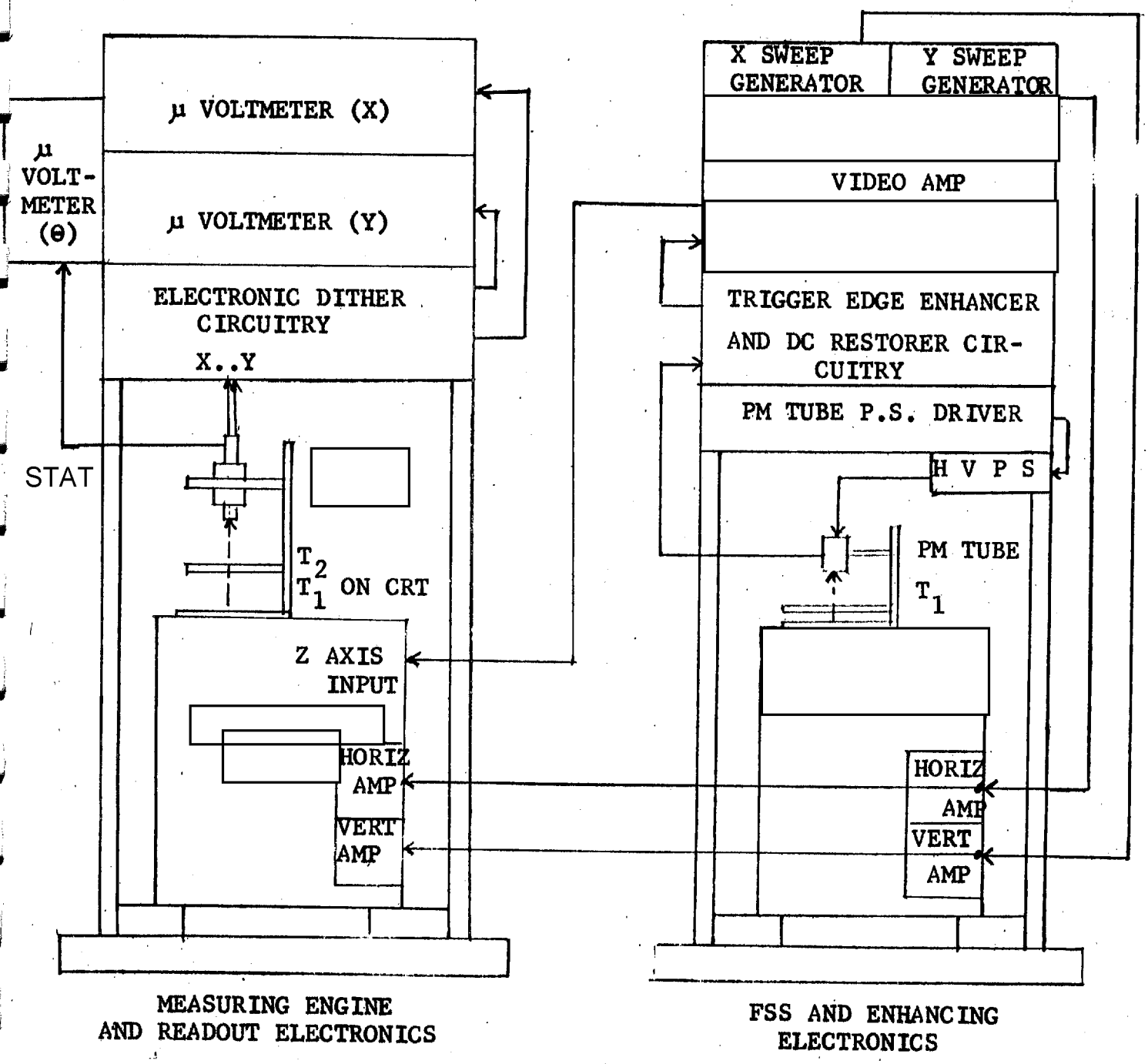

GENERAL PURPOSE OPTICAL CORRELATOR ASSEMBLY

FIGURE D-10

DITHER OUTPUT VS. DISPLACEMENT OF IMAGERY

RANDOM CHECKER PATTERN

PRODUCT MATCHING

TRANSPARENCY VS. TRANSPARENCY WITH A DIFFUSE INCANDESCENT LIGHT SOURCE

DATA TAKEN FROM EQUIPMENT TYPICAL OF FIGURE 5.

FIGURE D-11

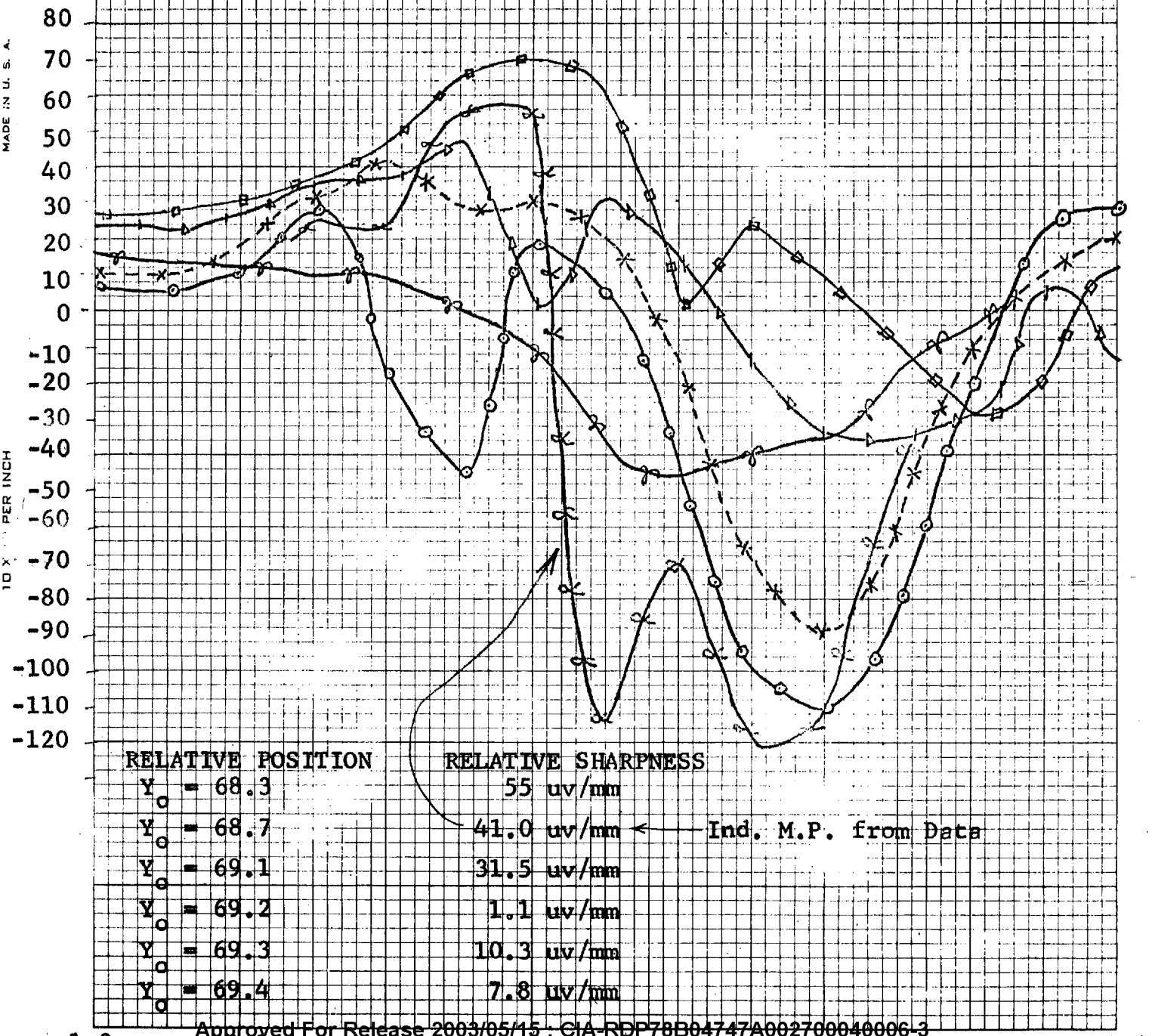

RELATIVE POSITION	RELATIVE SHARPNESS
Y_o = 68.3	55 uv/mm
Y_o = 68.7	41.0 uv/mm ← Ind. M.P. from Data
Y_o = 69.1	31.5 uv/mm
Y_o = 69.2	1.1 uv/mm
Y_o = 69.3	10.3 uv/mm
Y_o = 69.4	7.8 uv/mm

its positive mate to produce a bright spot (product match). The top transparency was mechanically and manually dithered in order to obtain ΔV_y data. The best approximation of the combined X, Y and θ match (correlation) point was found by eye. The X axis drive was locked and displacements on Y axis ($\pm$ 1.6 mm) and θ sense (5°) were made. Data was taken at various intervals in Y displacement at two angular positions (θ = 0°, and θ = 5°). ΔV_y quantities were computed by subtracting the V_y reading with dither from V_y with no dither at each point of axial displacement:

$$\Delta V_y = V_{y_o} - V_{y_\theta}$$

In most instances readings were taken every .2 mm increment in Y displacement. This dither data (ΔV_y vs. Y) is plotted for six different fixed X positions, five more or less off the X match position. One curve falls very close to being on the position of maximum correlation (i.e., true match position). This is indicated by the —α—α—line in Figure D-11. It is interesting to note that this curve possesses the greatest excursion, the greatest relative sharpness, and crosses the Y axis very near the origin. It also features nearly symmetrical false match point saddle regions. Figure D-12(a) is a photograph of the imagery.

Results of a study using real imagery with the first field presented on a CRT and correlated with a second field on a scaled down transparency is presented graphically in Figure D-13. Both transparencies were on [ ] (non-diffusive, very high contrast) film of a second generation. Figure D-12(c) is a photograph of the imagery which is constituted by fields, hills and valleys. This imagery was scanned and presented on the modified [ ] CRT [ ] face. The apparatus used is illustrated by Figure D-4 and associated written description. The display was compared with its negative mate to produce a dark spot in quotient match. The dither output (i.e., no dither-dither) readings are plotted versus lateral

STAT
STAT
STAT

(a) Random Checker Pattern

(b) River Scene - Stereo Pair

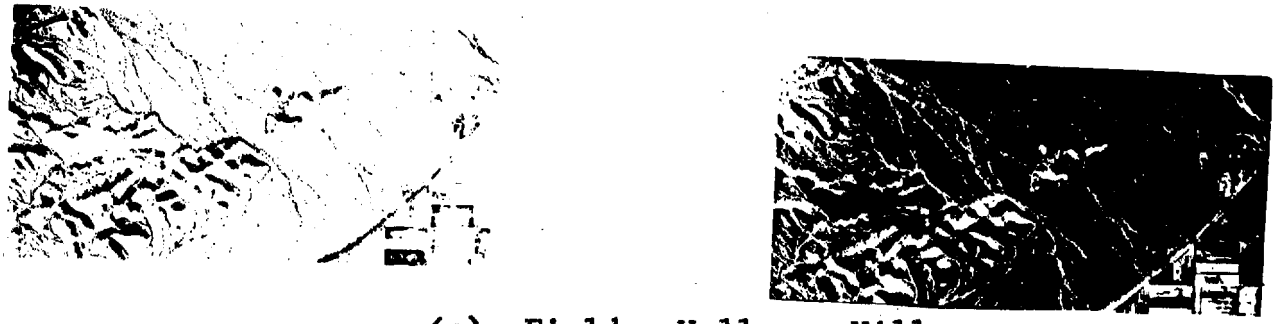

(c) Fields, Valleys, Hills

SAMPLES OF IMAGERY STUDIED

FIGURE D-12

DITHER OUTPUT VS. DISPLACEMENT OF IMAGERY
QUOTIENT MATCH

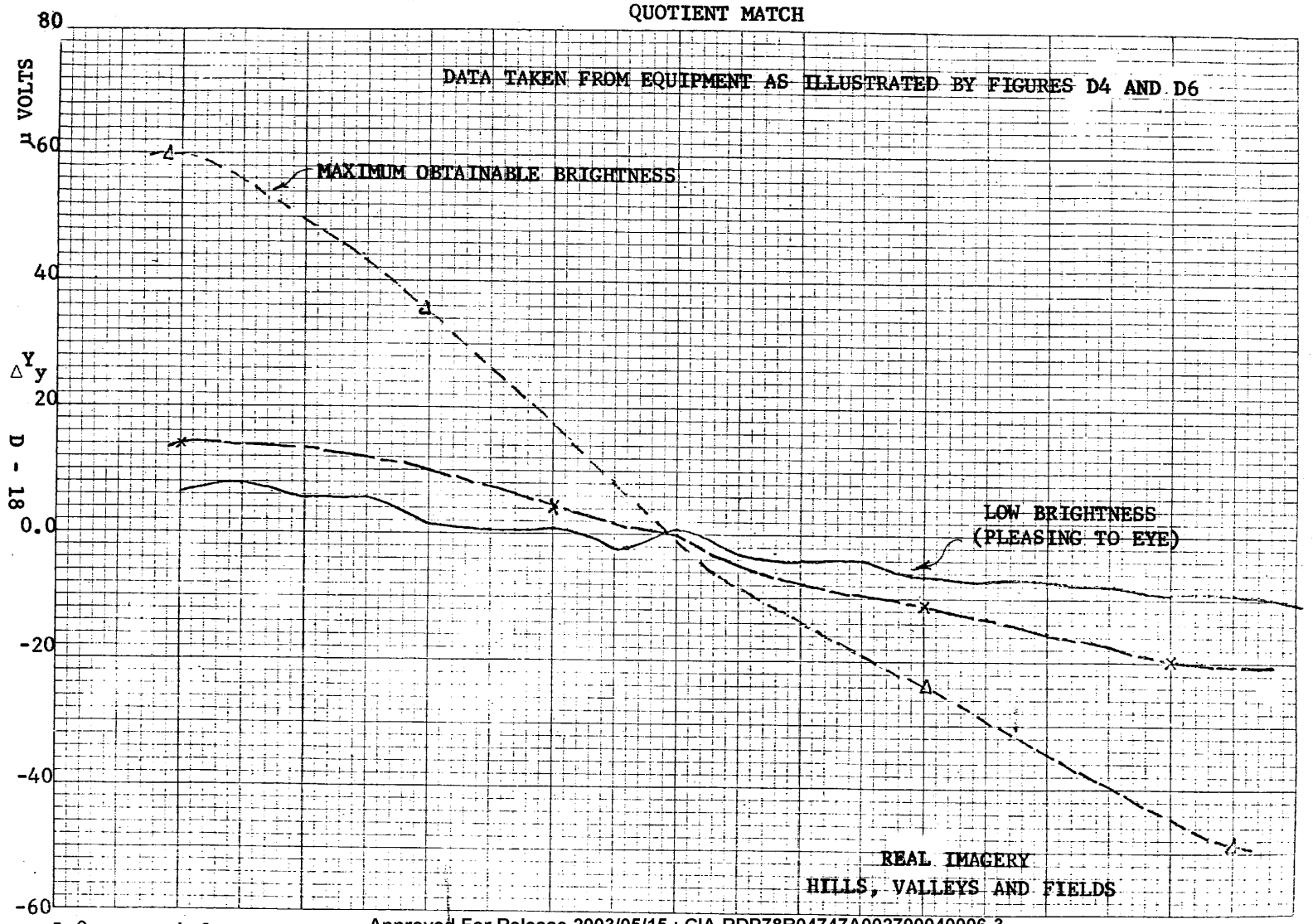

FIGURE D-13

(Y) displacement. Each curve represents a different CRT brightness.

Stereo pair mates with about 60 per cent common imagery were compared next. The results are presented as Figure D-14. Negative imagery on the CRT face was correlated with scaled down positive imagery on a film transparency. The apparatus of Figure D-4 was used. Since this was quotient matching, a black spot was produced. Some penalty in performance is inherent in this data due to the facts that the original imagery was (a) at least second generation, (b) on diffusive emulsion, and (c) converted to [ ] STAT [ ] copy was scanned and displayed on the CRT [ ] STAT face. It was compared to its stereo mate also on [ ] film in STAT quotient match. The correlation dark spot was generated within lock-on limitations imposed by the [ ] photocathode face, i.e., STAT $<\pm$ 2.5 mm of the optical axis. Dither output (no dither-dither readings) is plotted versus lateral (Y) displacement. Each curve represents a different average CRT fact brightness.

D 4. Limitations of Apparatus and Proposed Improvements

The measurements discussed in Section D-3 and other tests indicate the presence of several shortcomings. One is that use of diffusive film media degrades the results severely. A second is that for phosphor displays of small dark images, further intensification will be necessary for good performance. Third, these devices are sensitive to light leaks and re-reflections. The light leaks and re-reflectance problem has not been serious and can be minimized by good optical practices such as blackening mounting elements and the introduction of hoods and shields.

The image intensification problem can be alleviated by introducing an appropriate image intensifier tube plus accessories into the system of Figure D-10. The scheme of Figure D-7 is one implementation of this philosophy.

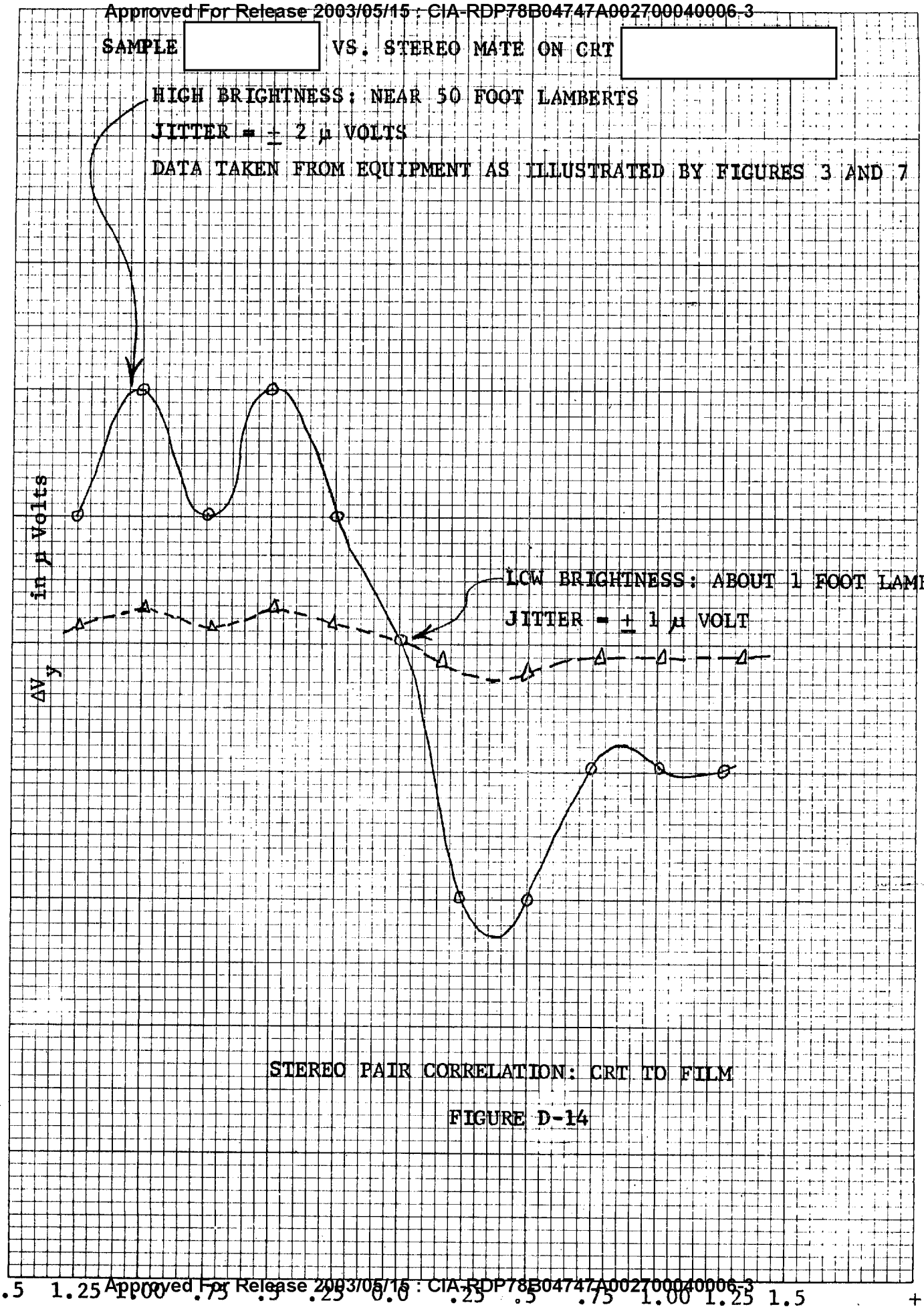

FIGURE D-14

Compensation for imagery on diffusive media is the most formidable problem. It is true that conversion of all imagery to a [STAT] equivalent is a possible solution. However, this is time consuming and expensive in film and photographic processing labor. Another and hopefully successful approach is to employ electronic techniques to compensate for diffusive imagery [STAT] triggers and high pass filters in cascade (differentiators and double differentiators) are being considered singly and in combination in order to produce the [STAT] effect" electronically. Initial tests of these devices indicate that the general idea has considerable merit. Activity in this direction continues. Using the partially assembled optical correlator system of Figures D-8, D-9, and D-10 tests were made involving the video processing chain. All results were limited for lack of a good wide band video amplifier matched to the system. However, the following improvements over straight non-processed video were noted:

With a high speed trigger effective contrast was definitely improved. Imagery was either black or white with very little gray apparent. Likewise, little detail was apparent.

With a high pass filter (single differentiation) following the video amplifier, the detail was greatly improved. Edges were more clearly defined giving the display a "3-D" effect. Contrast was similar to unprocessed video.

The use of a high pass filter plus high speed trigger in the chain resulted in less detail than with the filter alone but more than with the trigger used alone. Contrast was improved again, with only black and white levels displayed. Detail and edge sharpness was improved in this instance (river scene of Figure D-12) by reducing

the capacitance in the high pass filter. Much greater detail is expected when a wide band video amplifier becomes available and is put into service. It is expected that a combination filter-trigger subsystem will be developed which will effectively permit diffusive imagery to be used as a source directly without need for [ ] conversion. STAT

D 5. Capabilities

D 5.1 Metrological

The combined equipments provide a capability to scan 65 mm in the X and 35 mm in the Y directions and to measure the X and Y coordinates of fractional millimeter elements of an image on photographic plates or films. Both drives are manual. Motor driving capability for both axes can be quickly provided. Rotational capability for mechanical dither up to ± 20 degrees arc is provided.

D 5.2 Photometric

The combined equipments provide for the photometric capability to function properly (in the correlator sense) with image of density up to 3.0 density using diffuse incandescent tungsten illumination.

In the CRT to transparency mode photometric capability will accommodate imagery of density up to 2.0 density. Higher density ranges can be accommodated by use of the appropriate image intensifier tube.

D 5.3 Viewing

Operator viewing while seeking the correlation spot and its position is presently done with a rear projection screen which is manually inserted. The [ ] is then inserted following the removal of the viewing screen. A beamsplitting arrangement which will permit viewing while operating can be provided. STAT

D 5.4 Alignment Function

The combined equipments will provide for comparing two fields of imagery with 50 per cent (stereo pairs or other imagery), or more, common information. The fields can be displaced relative to one another (on the optical axis) as much as ± 2.5 mm and still permit spot within the lock-on limit. Alignment can be accomplished by moving one field relative to the other so as to place the correlation spot on center of the viewing screen or [ ] STAT photocathode, both being on the optical axis. Automatic field alignment can be provided for with some additional development effort.

D 5.5 Scale Adjustments

Adjustments in display size in order to match scale (or reduce scale) of one field relative to the other can be accomplished either by electronic (raster shrinking) or mechanical (lensless configuration) means.

STAT

D 6 [ ] Spot Position Sensor

[ ] the sensor for an STAT optical correlator was briefly examined. Using an incandescent tungsten light source with opal glass type diffuser, a small bright spot was generated and moved across the [ ] photocathode. STAT The nature of the study apparatus is illustrated by Figure D-15. [ ] was mounted and aligned rotationally on the X-Y transit STAT table. The light spot remained fixed and [ ] was moved accor- STAT ding to the table movement effectively moving the spot of light over the photocathode. Results were as follows:

For a fairly large spot (of about 0.1 inch diameter) and average light brightness at diffuser of .8 foot lamberts the data obtained is presented in tabular form below:

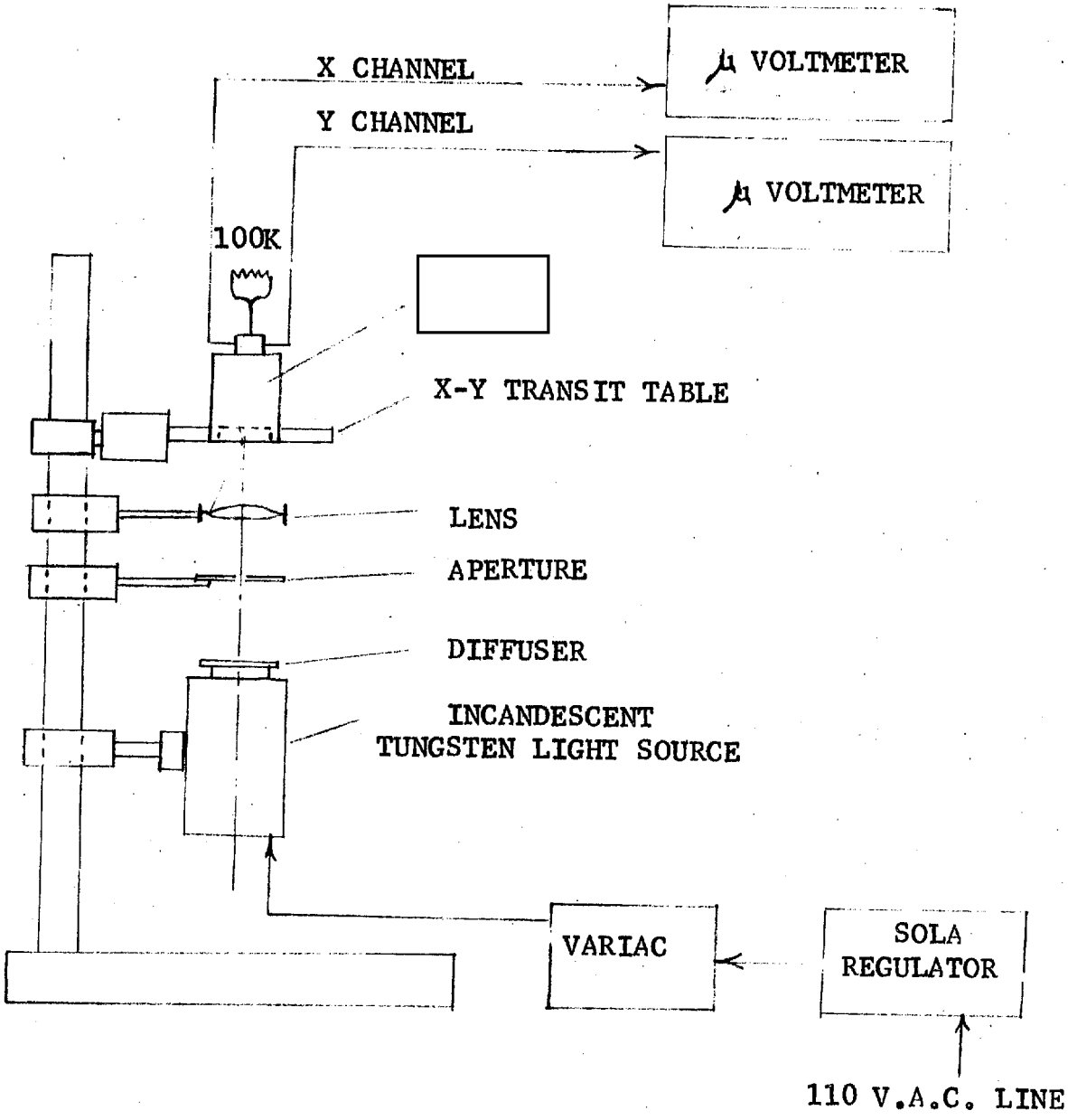

STAT

PERFORMANCE TEST EQUIPMENT

STAT

FIGURE D-15

Spot position (X-direction) from [ ] center	Output X channel
-2 mm	-2 mv
0.0 mm	0 mv
+2 mm	+2 mv

STAT

Spot position (y-direction) from [ ] center	Output Y Channel
-2 mm	-3.2 mv
0.0 mm	0.0 mv
+2 mm	+0.8 mv

STAT

Although there was some obvious crosstalk and asymmetry the response to spot movement was as expected. Outputs varied from a plus voltage through zero voltage near geometric center to a negative voltage as the spot was moved across the [ ] face. Total spread in each axis was 4 mv and response was approximately 1 mv/mm in each instance.

STAT

Using the same spot and by inserting neutral density filter media in the optical path, the reduction in signal excursion due to average density of imagery was predicted.

Film Density (Simulated) Neutral Density	Output Excursion Maximum Across [ ] Face (in millivolts) along X-Axis
0.0	0.0 ± 3 mv
0.7	0.0 ± 1 mv
1.4	0.0 ± 0.35 mv
2.1	0.0 ± 0.17 mv
2.8	0.0 ± 0.095 mv

STAT

Background level reading due to ambient light and electrical pickup was .018 mv. Stability at each point of reading was ± 2.0 μv.

Using increased brightness at diffuser surface of about 1.0 foot lambert an an effective spot size which could have been as small as .0015 inches but less than .015 inches looking through a medium of 0.0 to 0.05 density (glass plate) the following data was taken:

Spot Position (X Direction) from [redacted] Center	Output X Channel
-2 mm	+ .2 mv
-1.5 mm	+.145 mv
-1.0 mm	+.080 mv
-0.5 mm	+.04 mv
0.0 mm	0.0
+0.5	-.065 mv
+1.0	-.130 mv
+1.5	-.170
+2.0	-.200 mv

STAT

Spot Position (Y-Direction) from [redacted] Center	Output Y Channel
- 1.5 mm	+ .115 mv
- 0.5 mm	+ .072 mv
- 0.25 mm	+ .032 mv
0.0	0.0
+ 0.25 mm	- .03 mv
+ 1.0 mm	- .069 mv
+ 1.5 mm	- .118 mv
+ 2.0 mm	- .165 mv
+ 2.5 mm	- .192 mv
+ 3.0 mm	-.205 mv

STAT

In view of the data it would seem that for small spots, the source brightness will have to be increased to about 10 foot lamberts in order to handle imagery of up to 3.0 density.

A brief study of the [redacted] response to various CRT phosphors was made. Results showed that the emission spectra [redacted] had the most in common with the [redacted] spectral response. This includes all known phosphors including the [redacted] improved [redacted] [redacted] Compared to the diffuse incandescent tungsten light source (2900°K), the relative signal strength obtained from the same measured brightness of [redacted] radiation was fifty times less. This implies that in order to obtain equal signal levels from a [redacted] display system a light level gain of fifty times will be required. The answer is already available in the form of an [redacted] image intensifier tube using a [redacted] photocathode and a [redacted] display face. Low noise level gain of this device is about 60:1. It is small and will fit into most optical systems with ease.

STAT STAT STAT STAT STAT STAT STAT STAT STAT STAT STAT

D 7 Summary of Features and Capabilities

The Optical Correlator combinations produced to date possess the following capabilities and features.

1. Alignment of stereo pairs not displaced in excess of ± 2.5 mm relative to one another is possible. Angular lock-on requirement is ± 5 degrees or less.

2. Comparison of reconnaissance imagery is a present capability. Small area scan capability can be provided for detection of non-correlatable sub-regions.

3. Single plate pair correlation studies can be made presently. These could include terrain photos, X-ray photos, fingerprint comparisons, any other information fields presentable on film or plate transparencies.

4. Contrast and edge enhancement devices for making imagery on diffusive media more usable are available. Although electronic high pass filtering techniques show considerable promise for this purpose, use of optical spatial filters for edge enhancement in this regard can also be considered.

APPENDIX E

ANALOG CORRELATOR

E 1 Theoretical Justification

The purpose of this Appendix is primarily to report on the state of the hardware which has been assembled to permit testing of the Analog Correlator in the second half of the study program. It has not yet been possible, within the scope of the program, to prepare a full discussion of the correlation problem at a practical engineering level. What follows, therefore, is submitted as a minimal explanation of the theoretical basis for the Analog Correlator.

The classical expression for degree of cross-correlation between two time-varying functions $f_{a(t)}$, $f_{b(t)}$ is given by:

$$(1) \qquad AB = \frac{1}{T}\int_0^T f_{a(t)}\, f_{b(t-\tau)}\, dt,$$

where τ represents an arbitrary time difference between the two functions and T represents a sampling period. τ can be interpreted as a variable which permits the shifting along a time axis of one signal, or waveform, with respect to the other until a "best match" is achieved. It can be seen that the equation provides an interpretation of "best match": it is that relationship which maximizes the time integral of the instantaneous product of the two functions when that integral is divided by the sampling time itself.

From this it follows that if $f_{(a)}$ and $f_{(b)}$ are repetitive, and the time is allowed to approach infinity, then for any integral of instantaneous product which cycles between limits but retains an average value of zero over the repetition period, the correlation

function will approach zero. On the other hand, if the integral of the instantaneous product is non-zero at the end of a single period, the equation states that the correlation function will approach that value with diminishing variation as the time interval approaches infinity. Expressed in more prosaic terms, a storage device at the output of an analog computer performing the indicated mathematical value would assume a DC voltage indicating degree of correlation between the two signals.

In the case of a photogrammetric correlator using flying spot scanners, the video signals coming from two transparencies being scanned can be considered to be the functions $f_{a(t)}$ and $f_{b(t)}$. The signals are repetitive, at least in the case where the transparencies are stationary in the scanning fields. If, for simplicity, it is assumed that scanning occurs along a single axis, it is intuitively evident that a shift in spatial position of one transparency along that axis is equivalent to a variation of τ in equation (1). Therefore, if any correlatable information exists, one of the transparencies can be shifted until the correlation signal is at a maximum. That is, a "best match" can be secured. (It is unlikely that either the preceding or following statements would survive a test for mathematical rigor, but this is not the purpose of the present discussion).

A system which mechanized the correlation equation in its basic form would not be suitable for automatic closed-loop control, because it does not provide a convenient means of determining the sense and magnitude of an error. What is required is a system which produces zero output at maximum correlation, with positive or negative outputs indicating direction and magnitude of error for deviations from the best match position.

At this point it is convenient to assume that the two video signals represent identical imagery, though this implies auto-correlation rather than cross-correlation, and therefore does not truly represent the general case of arbitrary stereo pairs. Granted this license, however, it is clear that when the transparencies are in the matched position corresponding terms in the Fourier expansion of the two identical video signals will also be identical in phase and amplitude. It is now possible to take advantage of the fact that if a sine and cosine function of the same frequency are multiplied together, the average value of the product is zero. Expressed in another way, if a sine wave is shifted in phase by 90 degrees, the product of the original signal and the phase-shifted signal is zero.

Mechanization of this technique proceeds as follows: a network is synthesized which has the property of accepting a complex waveform $f_{(t)}$ and producing two outputs. One output can be expressed as $f'_{(t)}$. It differs from the original $f_{(t)}$ because the phase relationship between input and output varies as a function of frequency in such a way that the waveform is not preserved. This is true for any network in which the phase shift is not a linearly increasing function of frequency, but the distortion of this output is only an incidental property of the network. The significant property is that the second output exhibits a 90 degree phase shift with respect to the first one, for any frequency within the operating band.

It can be seen that, in the matched position of the transparencies, if output #1 of the channel A network is multiplied by output #2 of the channel B network, each frequency present in the complex

signals will produce a zero average product. The same is true when output #1 of the channel B network is multiplied by output #2 of the channel A network. Therefore, at the position of best correlation the outputs of the multipliers are at zero, which is the desired condition.

Recalling that a spatial shift of either transparency is equivalent to changes in the relative phases of the frequency components in the two channels, it is apparent that such a displacement will upset the quadrature relationship between signal components entering the multipliers, and therefore will cause a non-zero output. For idealized, simple, cases it is readily shown that the sign of the output reflects the sense of the error. Investigation of signal behavior under practical cases is the object of the present study.

Finally, it is noted that the hardware implementation described in the next section is, for practical reasons, actually the difference of two correlation functions:

$$(2) \quad e = \frac{1}{T}\int_0^T f_{a(t)} f_{b(t-\tau)}\,dt \quad - \frac{1}{T}\int_0^T f_{b(t)} f_{a(t-\tau)}\,dt$$

E 2 Hardware Status

The system block diagram is shown in Figure E-1. Two video signals, A and B, are applied to two phase-shifting networks which operate upon them as described above. The outputs are amplified and inverted to yield the complementary signals needed to drive the multipliers. The multipliers produce the cross-products described above, with one producing an inverted output to

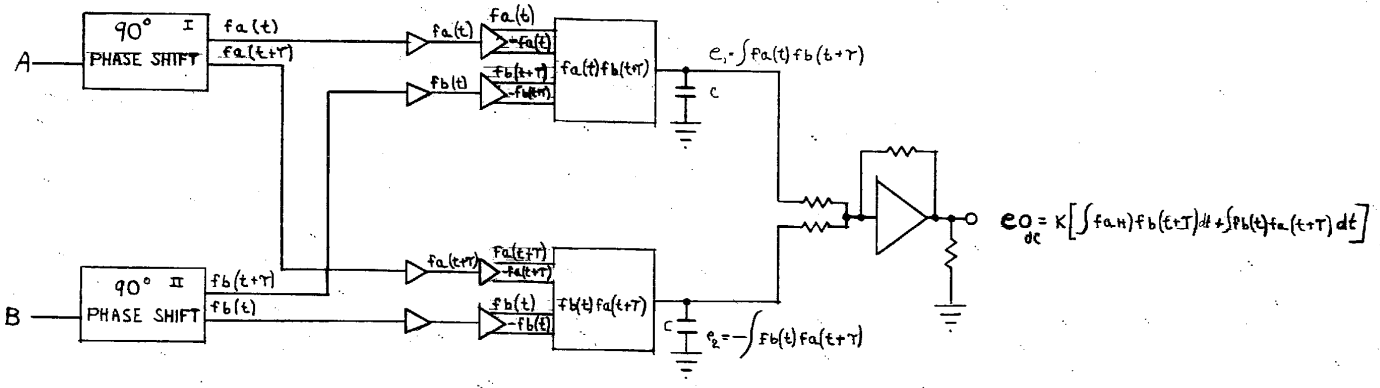

ELECTRONIC ANALOG CORRELATOR SYSTEM

FIGURE E-1

serve as the negative term of equation (2). The multiplier outputs are then integrated and summed in an operational amplifier whose output is the correlation error signal.

A plot of the system response to two sinusoids of equal amplitude and frequency, but differing in phase, is shown in Figure E-2.

E 2.1 Phase Shift Network

The phase shift network is a lattice type L-C circuit used to provide a constant 90 degree phase shift between the output pairs of the network. The plot of the output pairs $f_{a(\gamma)}$ and $f_{a(\gamma + 90°)}$ with respect to the input as shown in Figure E-3. The attenuation of each output with respect to the input is shown in Figure E-4.

The circuit diagram is shown in Figure E-5. The network has been designed to perform the constant phase shifting function for a band from 50 Kc to 5 Mc. This bandwidth has been intuitively selected as the probable range of maximum information based on the scanning system tentatively selected for use to supply the video information.

E 2.2 Correlator

The electronic correlator used in this system is a four quadrant multiplier and integrator (Figure E-6). The output yields a voltage analogous to the similarity between the incoming signals as a function of phase shift between them. It is described in Electronic Industries, August 1965, in an article by A. N. Stoll. There it is explained that the resultant output can be simplified to:

$$e_o = \frac{4K}{RC} \int_o^T A \cdot B \, dt.$$

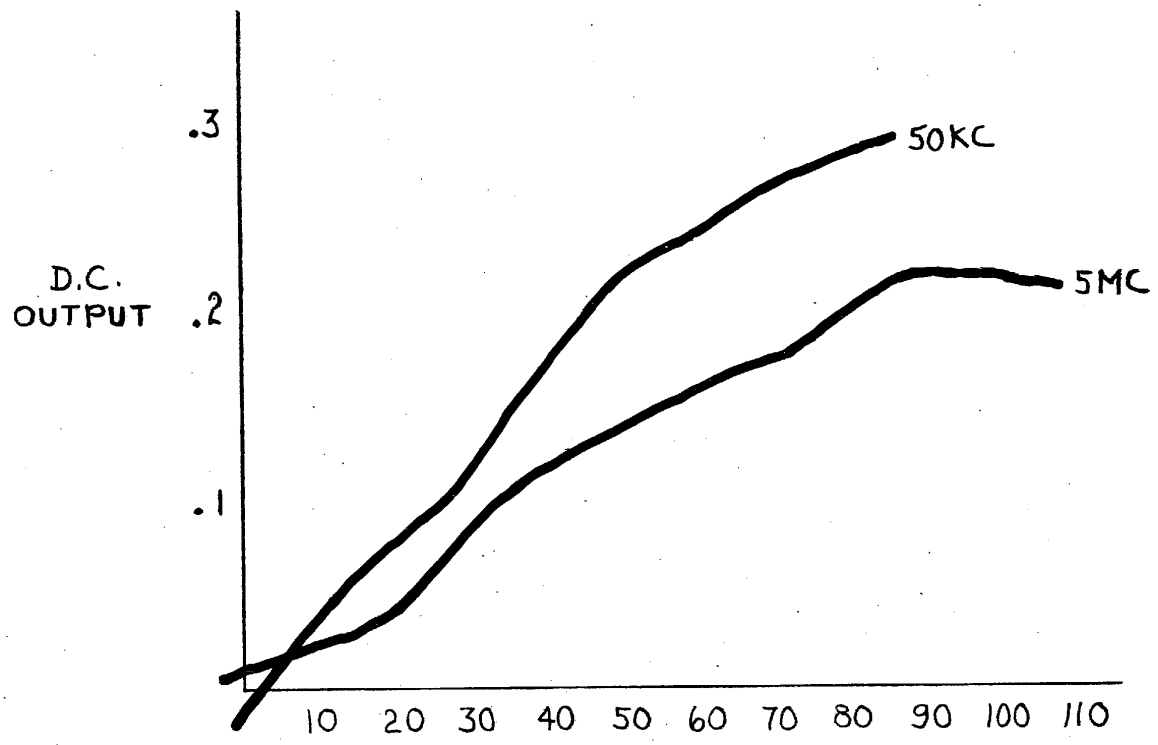

FIGURE E-2

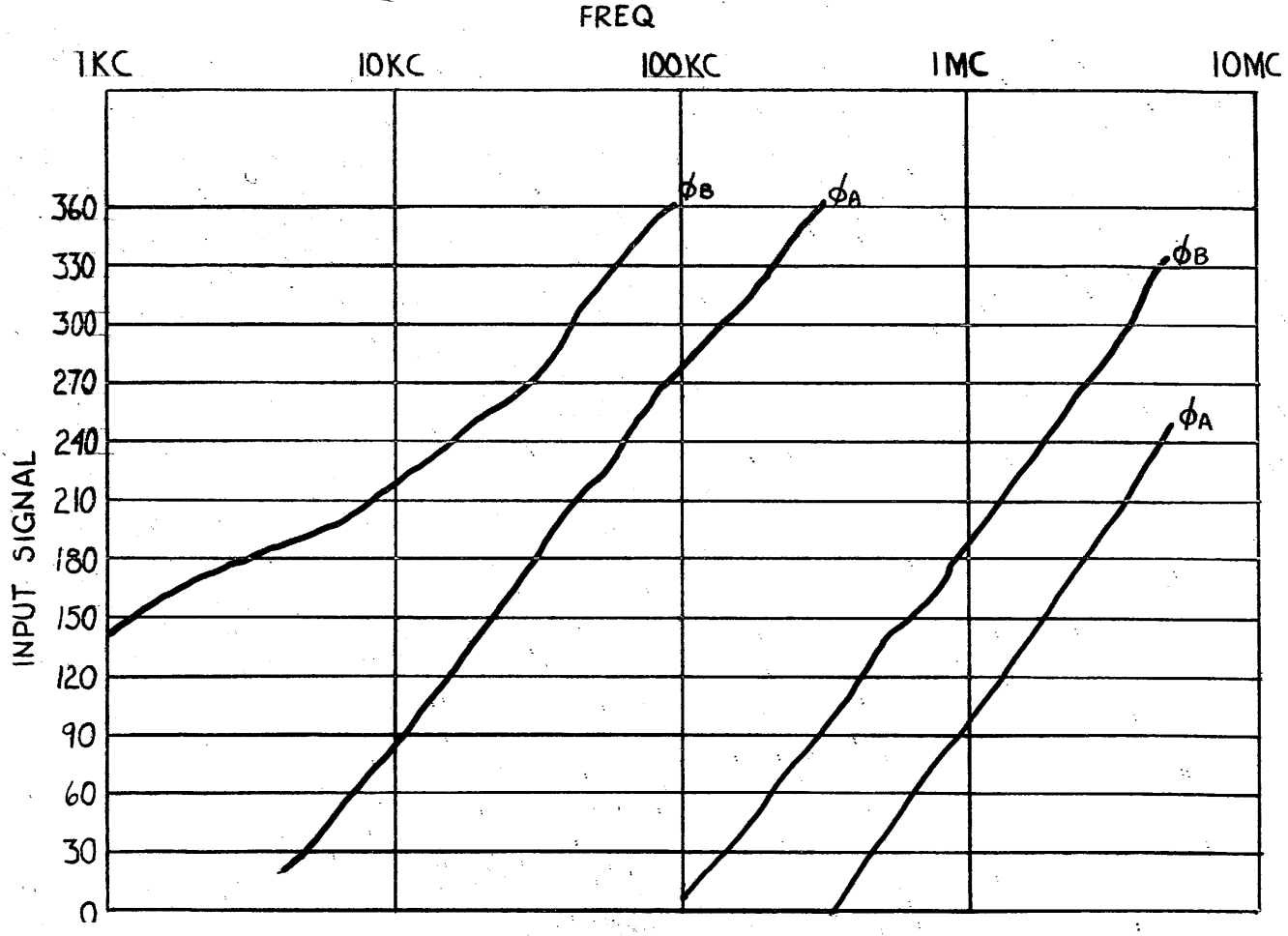

PHASE SHIFT AND PHASE OUTPUT WITH RESPECT TO INPUT SIGNAL FOR L-C PHASE SHIFT NETWORK

FIGURE E-3

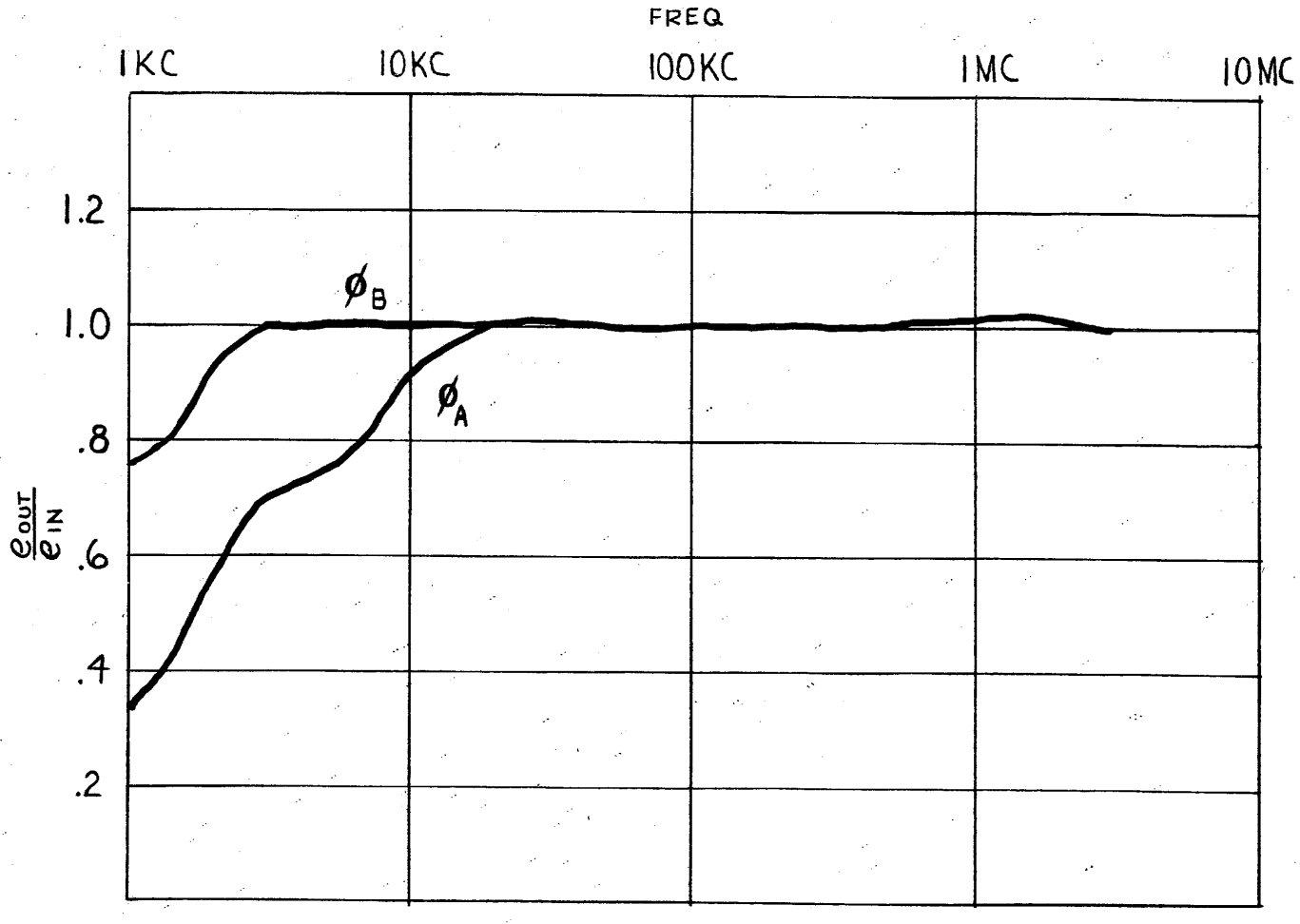

RATIO OF E_{OUT} (PHASE A AND PHASE B TO E_{IN} VERSUS FREQUENCY FOR L-C PHASE SHIFT NETWORK

FIGURE E-4

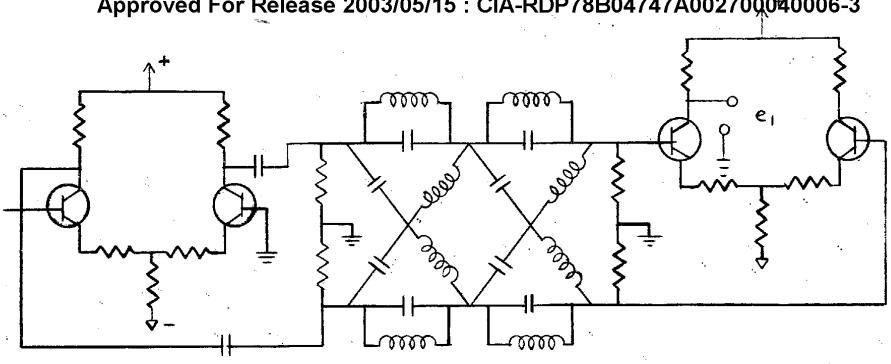

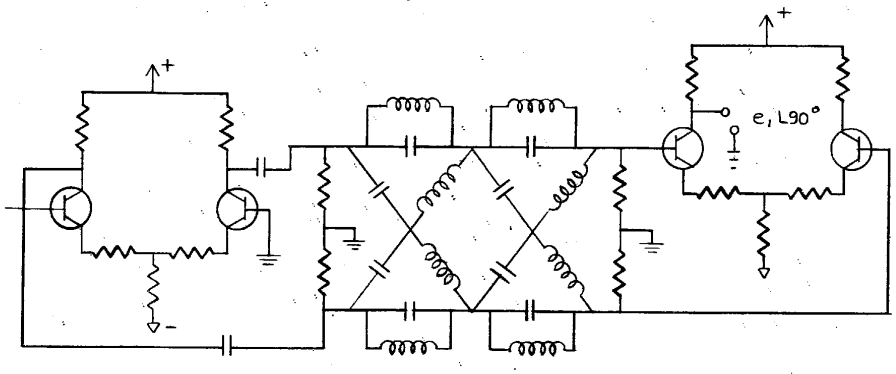

90 DEGREE PHASE SHIFT NETWORK

FIGURE E-5

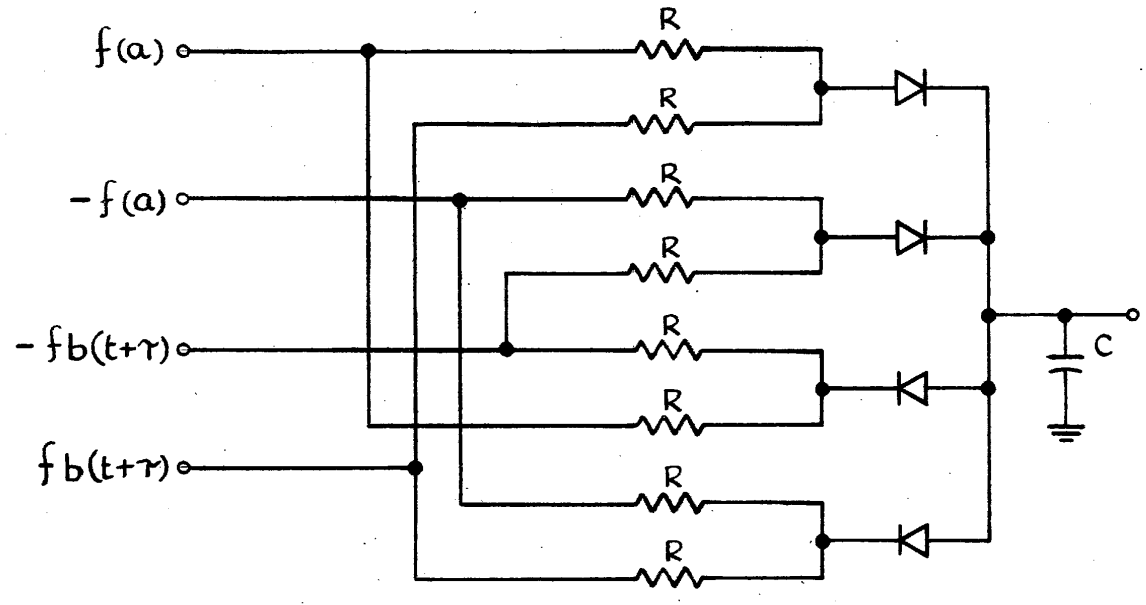

CORRELATOR

FIGURE E-6

In the circuit, no attempt is made to operate the diodes in their square law region. Their outputs may be closer to linear than square law so that the current-voltage relationship is given by $i = K_1(A+B)$ instead of $i = K_2(A+B)^2$. This alters the behavior of the circuit in detail only. A plot of the output of one correlator network as a function of the change in phase between two equal frequency sinusoids is shown in Figure E-7.

E 2.3 Amplifiers and Phase Split Amplifiers

The amplifers used in this system are straightforward current feedback amplifiers yielding a gain of ten (See Figure E-8). Emitter followers have been used for coupling purposes to reduce the effect of loading. The correlator circuit was intended to be driven by transformers but due to a delay in parts delivery, a substitute phase inverter amplifier was used to generate the push-pull effect.

E 2.4 Subtractor

The subtraction of the outputs from the correlators is actually accomplished using an operational amplifier as a summing device. Reversal of the diodes in one correlator provides the opposite polarity at one output, hence the addition of these two signals is effectively subtraction of these outputs.

E 3 Conclusion

While it is premature at this point to conclude that the analog correlator will provide the proper results using video signals, an optimistic view has been taken based on the existing data. In the following weeks, it is intended to introduce video information into the correlator in an actual tracking system. Additional switching circuitry will also be necessary in order to integrate the correlator into this tracking system due to particular requirements of the scanner operation.

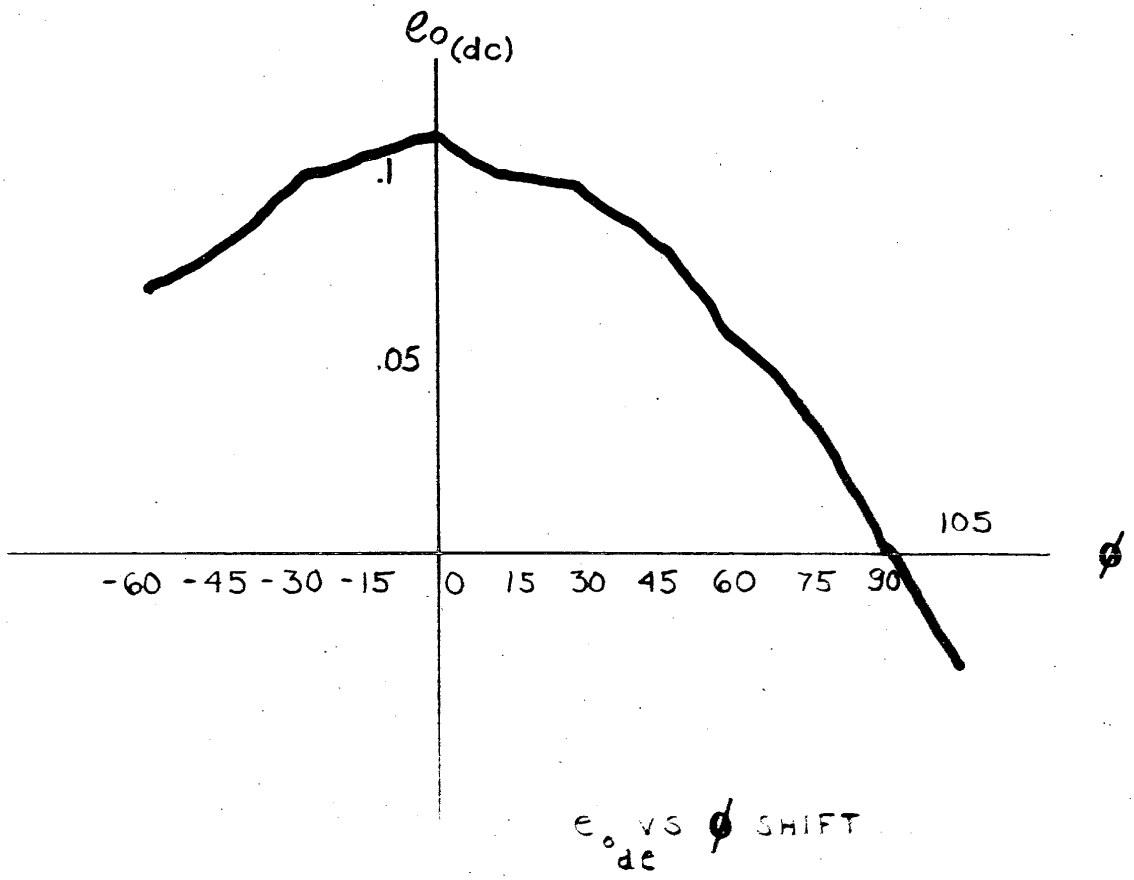

CORRELATOR OUTPUT

FIGURE E-7

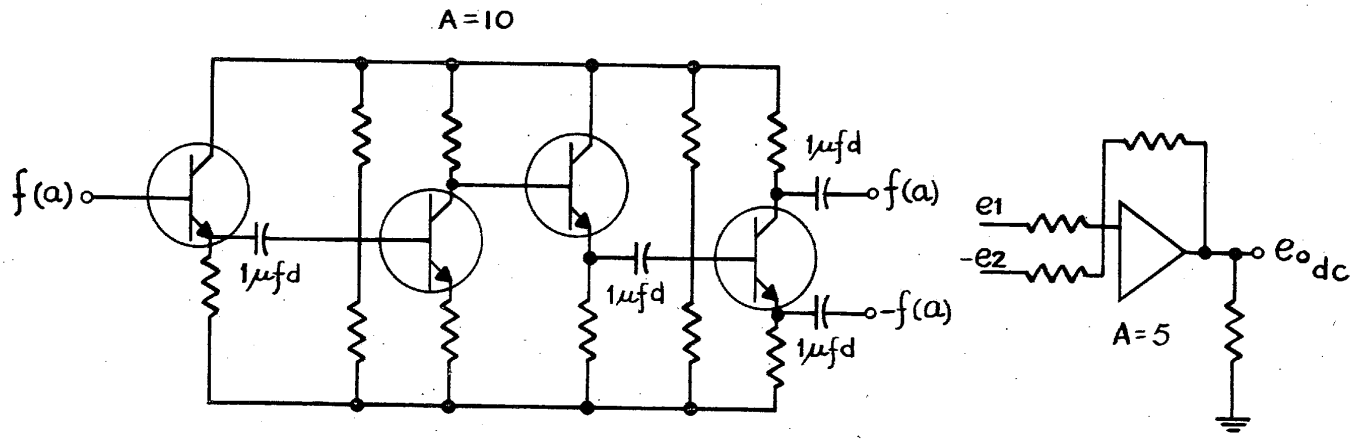

PHASE INVERTER AND AMPLIFIER

SUMMING AMPLIFIER

FIGURE E-8

APPENDIX F

HIGH PRECISION STEREO COMPARATOR METERING SYSTEMS

F 1 [ ] STAT

F 1.1 Description

The [ ] System consists of two units: (1) the transducer or sensing mechanism, and (2) the associated electronics package. STAT

The transducer unit consists of a pair of glass plates separated by a small air gap allowing capacitive coupling to occur. Facing surfaces of the plates are coated with metallic patterns. One plate (coupler) is mounted on the element whose position is being measured; the stationary plate (driver) is mounted on the supporting structure and contains all electrical connections.

The electronics package provides the signals which energize the transducer, measure the phase shift, digitize the result and display the readout. Input to the transducer is composed of four sinusoidal signals of a given frequency with a quadrature phase relationship. Each signal excites a particular portion of the "Driver" pattern. These four signals are capacitively coupled to the "Coupler" plate where they are vectorially summed. The resultant is a constant amplitude signal whose phase is directly proportional to the change of position of the "Coupler" plate with respect to the "Driver" plate. This phase-shifted information signal is then capacitively coupled back to the "Driver" plate and processed by the system electronics.

Processing and digitizing are accomplished by comparing, in real time, the phase-shifted output signal with the input or reference signal. The reference signal starts a high-speed counter, with counting of the pulses continuing until the phase-shifted transducer output signal stops the count. When this termination occurs,

the digital information in the counter represents the linear position of the system. Coarse position is sensed by a brush-type encoder or other suitable means. It is stated that the interrogation rate can be several thousand cycles per second.

The driver and the coupler, for a ten-inch measuring range, will be twenty and ten inches long respectively. For a twenty-inch measuring range, the driver will be thirty inches long and the coupler ten inches long. The cross section of the coupler and the driver will be approximately one by two inches with electrical connections at one end of the driver.

The air gap must be between 0.002 inches and 0.011 inches and must remain constant to within 5 per cent. The absolute accuracy is estimated to be one micron in 250 millimeters. (See Section F 1.2) Inaccurate table motion, as it affects the air gap, will result in a cyclic error. No estimate of air gap change versus resultant error was available. Lateral motion that does not change the air gap will not cause a significant error.

Power requirements are very low - approximately one watt per axis with zero watts dissipation at the transducer.

F 1.2 Discussion

[ ] successfully applied the basic principle to angular encoders of one arc second resolution and absolute accuracies of 4.0 arc seconds or better. They do not have an off-the-shelf angular or linear [ ] Each system has been custom-designed and it was stated that all future systems will be handled the same way. STAT STAT

The linear [ ] breadboard that was demonstrated was very massive. The driver was approximately two inches thick, six inches STAT

wide and twenty-four inches long; the coupler was similar in cross section and approximately ten inches long. Three sliding feet attached to the coupler maintained the air gap while two additional sliding feet restrained the coupler to straight line motion.

Accuracy of displacement was checked by use of calibrated gage blocks. The difference in length of gage blocks was measured by placing each block in turn between a spring-loaded, ball-end anvil on the driver and a ball attached to the coupler. Differences in readings from the [redacted] counter were compared with the calibrated gage block differences. STAT

Because of "stiction", it was difficult to obtain readings. An electronic height gage was utilized to obtain a null reading from the spring-loaded ball on the driver. The present set-up shows an error of approximately five microns in ten inches. The source of the error has not been resolved.

F 1.3 Conclusions

STAT [redacted] has several advantages and disadvantages STAT when compared to other metering systems [redacted] STAT [redacted] Among the advantages are:

1) No heat sources at the transducer [redacted] STAT STAT [redacted]
2) No mechanical moving parts [redacted] STAT
3) High interrogation rate [redacted] STAT
4) A least count of 0.1 micron [redacted] STAT STAT [redacted]
5) Absolute system [redacted] STAT

Some disadvantages are:

1) Very close air gap and gap tolerance [redacted] STAT
2) Considerably greater bulk than the other two systems.

3) Custom design required.

4) Uncertainty of accuracy from air gap variation.

Consideration of the advantages and disadvantages indicate that if the large size can be accommodated, the [redacted] System would be preferable to [redacted] metering systems. The above assumes that cost and delivery are not prohibitive and that necessary compromises are acceptable.

STAT
STAT

F 2 [redacted] Metering System

STAT

F 2.1 Description

[redacted]

STAT
STAT
STAT

The basic [redacted] system consists of three elements: a precision glass scale, a compact reading head and a remote display panel. In application, the [redacted] head and scale are mounted on separate machine elements, moving in relation to one another. The reading head scans the scale optically and makes absolute determinations of position, relative to a zero reference point on the scale.

STAT

STAT

[redacted] scales are glass-base replicas having reflective graduation marks spaced at one-millimeter or .050 inch intervals. Spaces are held to sub-micron tolerances while overall accuracies are controlled by sophisticated ruling and replication techniques. A separate series of decimal code tracks identifies each fine scale graduation used in the interpolation process. The graduations are protected from dust and damage by a layer of flat glass.

STAT

The [redacted] reading head contains a fine encoder or scale interval interpolator, as well as a coarse encoder which scans the decimal coarse code tracks on the scale. The pulse outputs of the two encoders are electronically processed for visual numerical display and for coded decimal output [redacted] makes new absolute measurements

STAT

every 100 milliseconds.

The fine encoder uses a simple but unique principle of digital interpolation. The interpolator contains a long-life light source, an objective lens, a beamsplitter and a null type photosensor capable of detecting the centers of the reflective graduation on the scale with sub-micron resolution. A rotating optical element scans a scale with a radius which is large enough to assure that at least two graduation marks are projected onto the graduation detector in each half-revolution. In circular motion, the linear displacement in a given direction is sinusoidal relative to angular displacement. By creating a sine-frequency-modulated pulse train, which is synchronous with the rotation of the scanning axis, it becomes possible to digitize the linear component of the scan in the measuring or "X" direction. This relationship gives a direct and absolute digital representation of displacement. The [ ] principle does not utilize first approximations, nor does it digitize voltages from analog transducers. STAT

[ ] embodies a unique sine-modulated pulse-train generator in which the key element is a rotating transparent disc having a parallel pattern of alternately opaque and clear rulings. This "clock disc" is rigidly attached to the same rotor which supports the scanning element. A light beam transmitted through the clock disc passes through a lens and is reflected back through the lens and clock disc by a mirror. A sensitive photodetector observes the passage of consecutive opaque and clear lines. Note that in a complete revolution, the frequency of passage of the lines will reach zero at two 180 degree-spaced stations on the disc and that two points of maximum frequency will be observed. Frequency is exactly sinusoidal relative to angular displacement, just as the X-displacement of the scanning axis is sinusoidal. STAT

The interpolated measurement is gated to start by an optical "start pulse generator" consisting of a fixed illuminated slit, a rotating lens mounted in the clock disc, and a fixed target-slit with a photodetector behind it. The "stop counting" pulse is generated by the null type scale graduation detector [ ] is calibrated at the factory by adjusting the radius at which the clock disc is scanned. The adjusting mechanism tilts a thin glass plate to produce a refractive offset. Similar glass "tuners" are provided for exact phase adjustments of the clock pulse system. These adjustments may be performed in the field if necessary.

STAT

[ ] coarse encoder consists of a long-life illuminator, a collimating and beamsplitting system, three photodetectors and a moving lens which scans the three reflective coarse code tracks on the scale. The moving lens is housed on the same rotor that carries the scale scanning element and the clock disc. The reflective lines in these tracks are imaged on the three photodetectors by the moving lens, thereby generating three decimal-coded pulse trains.

STAT

[ ] electronic console outwardly resembles an ordinary decimal counter but its internal functions are more specialized. Much of the circuitry is utilized for pulseshaping and for preventing ambiguity. The input from a metric [ ] fine encoder may consist of from zero to 1000 "micron" pulses. The counting logic permits a "carry" of one millimeter to the coarse encoding section when the fine encoder reading exceeds 999 microns. The output of the fine encoder also electronically modulates the angular position of the swinging lens at which the coarse encoder begins transmitting decimal pulses. Thus, it is impossible [ ] to read ambiguously or to drop a figure during a 999 to 1000 transition.

STAT

STAT

STAT

[ ] decimal display and memories are reset at 100 millisecond intervals. The typical observed randomness or inconsistency of interpolation is better than ±1/5 count (± ten millionths inch). Linearity of interpolation may be held to within one-fourth micron or twelve millionths inch. STAT

Because [ ] is a non-incremental system, the circuitry need not accumulate large numbers of counts. Accuracy is unaffected by power interruptions or stray pulses on the line [ ] cannot lose count after a fast traverse. Up to three measuring axes may be served by the same counter on a manually switched, or automatic time sharing basis. STAT STAT

Each [ ] axis may be preset to zero (or any other figure) at any point in its travel by means of digital switches. The absolute position of the floating zero point remains stored and displayed on the switches. STAT

[ ] is provided with self-contained calibration circuitry. In the "calibrate" mode [ ] pulse train is gated to start by the first scale graduation encountered by the detector and is stopped by the second graduation. The pulse count, as displayed in decimal form, is exactly equal to the scale graduation spacing. The method may be used to check the consistency of the spacing of the scale graduations, as well as the calibration of the head itself. A modified calibration procedure is used to check interpolation linearity. STAT STAT

F 2.2 Discussion

[ ] system can be easily produced having a least count of 0.5 micron. A significant increase in sampling rate does not seem feasible at present. If the least count is reduced to 0.5 micron and the sampling rate is acceptable, the [ ] system would be the least expensive metering system for the High Precision Stereo Comparator. It would, however, STAT STAT

still have the same limitation as other "between stages" metering systems such as the Moire Fringe [redacted] in that the overall system accuracy would be significantly affected by stage motion inaccuracies. One feature that is undesirable as compared to the [redacted] is that incremental inaccuracy could exceed the required accuracy since only individual lines on the scale are utilized for each position readout; rather than averaging over many lines.

STAT

STAT

F 3 The Moire Fringe System [redacted]

STAT

F 3.1 Description

The essential element of the measuring system is a length of optical diffraction grating having a line structure with a precisely-known number of lines per unit length. When one section of such a grating is superimposed on another, with the line structure of the one at a slight angle to that of the other, the integrated interference effects caused by the intersection of the individual lines gives rise to a Moire fringe pattern. This pattern has an approximately sinusoidal distribution of density and is, in effect, a greatly magnified version of the grating pattern, the individual lines being widely separated. When one grating is moved along the length of the other, the fringe pattern travels across the grating at right angles to the direction of movement. The width of one fringe can be made sufficiently large to cover the entire field of a separate section of grating 0.375 inch square; this grating section is referred to as the index grating.

If a beam of parallel light is projected through this field, then a relative movement of one line between the index grating and the long, or scale, grating will cause the field to go through a complete cycle of light intensity as the fringe travels across it. A photosensitive element, integrating the light over a section of this field, can be used to convert the changes in light intensity into fluctuations of electrical current. These signals, which will be

approximately sinusoidal in form, can then be used to provide, in either digital or analog form, an immediate and precise measurement of travel.

The direction of fringe pattern movement reverses when the direction of travel of the one grating relative to the other is reversed. In order to take direction of movement into account in the measuring system, it is necessary to view the pattern over at least two areas. These areas are so arranged as to make the density variation in one area 90 degrees different in phase to that of the other. The electrical output from photosensitive elements aligned with these two areas of field will thus have a quadrature phase relationship. This two-phase system contains complete and continuous information concerning the relative movement between index and scale gratings. The number of complete cycles, or fractions of a cycle, will indicate the total travel, the frequency will be a measure of the velocity of travel, and the direction of phase rotation will indicate the direction of travel.

Although only two phases need be created, it is found advantageous to divide the field into four equal areas. The angle at which the lines of the scale and index gratings intersect is referred to as the angle of skew and can be varied by rotating the index grating. By this means, the fringe pitch can be so adjusted as to result in output signals whose phases are 0°, 90°, 270° and 180°. The o° and 180° signals are subsequently combined in an amplifier which has a high discrimination in favor of anti-phase signals, the zero frequency and co-phasal components being greatly attenuated. The 90 degree and 270 degree signals are similarly treated. From these two pairs of signals, two vectors in quadrature are extracted, the size of these vectors being substantially unaffected by light source intensity, ambient light or variations in grating transmission.

F 3.2 Discussion

It was disclosed [redacted] that prismatic (250 lines/mm) gratings are no longer offered because of many problems experienced with them. A one micron system now uses a line-and-space Ronchi ruling of 100 lines per millimeter with electronic subdivision to a least count of one micron. STAT

The line placement is expected to be more precise with an expected accuracy of one micron in 200 millimeters through a distance of 6 feet. Because of the coarser ruling, the air gap is nominally .004 inches with a tolerance of ± 20 per cent. Packaging of the transducer is essentially unchanged while the electronics have been greatly improved with counting speed up to 100 KC. An operating system can be examined [redacted] STAT

Several systems are soon to be installed [redacted] within the next three months. STAT STAT STAT

F 4 Metering System Selection (Refer to Table F-1)

The development objective for the precision stereo comparator is to design and fabricate a system that advances the state of the art. Since a design goal for an accuracy of one part in 100,000 is specified, it is axiomatic that the metering system should contribute as little error as possible to the total system error.

The transfer of measurements from the metering to the optical axis is a basic problem. The difficulty is in designing engine ways that move in perfectly straight lines, orthogonal to each other and that are free of pitch, roll, and yaw. It is also impossible to completely remove deflection effects caused by the moving center of gravity.

A metering system that inherently reduces or eliminates the above problems is obviously highly desirable. Of the various systems considered, it becomes apparent that the interferometer as described previously (second monthly report) is the only one that fulfills these requirements.

Both [redacted] system are expected to have a scale accuracy of approximately one part in 250,000. The transfer of measurements to the optical axis invariably results in potential error from inaccurate stage motion since both systems are usually mounted off-axis and co-planar with the film plane or nearly on-axis but out of the plane of measurement. STAT

A recent improvement reported [redacted] makes the interferometer even more attractive. He stated that the system could be supplied with automatic correction for the effects of barometric pressure and temperature changes and with a readout in engineering units (to a lest count of 0.1 micron) instead of fringes or fractions of fringes. He is also using a two-megacycle reversible counter that he feels will easily accept the maximum translation speed of three inches per second. STAT STAT

TABLE F-1

METERING SYSTEM COMPARISON

STAT

Complexity of Assembly	Medium	Low	Medium	High
Maintenance Requirements	Frequent Adjusting	?	?	?
Accuracy	1:200,000	1:250,000	1:250,000	1:500,000 with auto. compensation for temp. & pressure
Least Count	1.0 u	0.5 u	.1 u	.1 u
Count Speed	3"/Sec	Unlimited	Unlimited	3"/Sec
Effect of Ambient	Low	Low	Low	Low (if corrected for)
Heat Output	Medium	Low	Zero	Zero, except at laser
Cost per 2 axes System	?	15K	50K to 75K	30K to 40K
Delivery	6 months	1 year	1 year	12-15 months
Assembly and Alignment Requirements	Critical	Not Critical	Critical	Critical
Effect of Inaccurate Stage Motion	Error can be first order	Error can be first order	Error can be first order	Error is second order
Effect of Cabling on Stage Motion	Significant	Significant	Significant	None-no cabling to Stage
Type	Incremental	Absolute	Absolute	Incremental
Knowledge of Position	Instant	Sampling Rate=10/Sec	Sampling Rate=1K/Sec	Instant

APPENDIX G

MATERIAL SELECTION CRITERIA FOR A HIGH PRECISION MEASURING MACHINE

G 1 Introduction

The parameters governing the choice of a material to be used in a high precision comparator are definite and measurable. Of paramount importance is the stability of the material with time, that is, the anticipated change in dimension resulting from internal stress systems or concurrent metallurgical instability. Other characteristics such as Young's Modulus of Elasticity as it bears directly on the load-deflection characteristics of the measuring stage, machinability and, where applicable, castability, corrosion resistance and its ultimate effect on time-reliability concepts of the equipment, the coefficient of thermal expansion and thermal conductivity of the materials, reproducibility as it applies to the ultimate machine configuration, the availability of pertinent data and the cost of the material are all factors that enter into such a selection. By a process of elimination, the choice can be reduced to a selection from the three following materials.

G 2 Meehanite Metals

Meehanite Metals are a family of cast ferrous materials containing free graphite.

The quantity and form of the free graphite imparts to the materials certain extremely desirable engineering characteristics. The particular grade selected for evaluation is a Type GA Meehanite. It is a general utility iron that can be readily cast. Because of its structural homogeneity it retains high dimensional accuracy in service.

Some of the physical properties of the material are:

Tensile Strength (psi)	50,000
Modulus of Elasticity (psi)	20×10^6
Compression Strength (psi)	175,000
Brinell Hardness (as cast)	>207
Thermal Conductivity, 50° - 450°F (BTU/HR/Sq Ft/Inch thick/°F)	350
Coefficient Thermal Expansion 100°F to 1000°F (per degree F)	7.2×10^{-6}

This material has a history of successful applications in the field of precision measuring equipment. Because of this, a clearly-defined technology has evolved from basic foundry practices to final scraping and lapping.

It has been found that casting stresses can be considerably increased or decreased by the foundry techniques involved. Uneven cooling rates due to different section thicknesses are the most potent source of casting stresses. Too rapid removal from the mould is another source. Thermal stress gradients can develop due to low pouring temperatures. Too high a dry strength of cores can induce stresses during the cooling cycle. Improper heat treatment and poor machining practices can and often do result in unstable parts. An awareness of these potential problem areas is the first step toward their elimination.

The utilization of silicon carbide at appropriate points in the mould can even the cooling rate. The silicon carbide has a much higher thermal conductivity than the normal sand mould and is therefore located around the heavier sections. Cooling the part in the mould to room temperature is obligatory. Heating the mould will induce "hotter pouring" and lessen the contraction stresses. Proper heat treatment procedures can be defined for optimum stress relief.

Typically [redacted] (Reference #1) STAT
manufacturers of the [redacted] precision jig grinder for the STAT
European market, utilizes special machining fixtures designed to avoid setting up stresses in the casting during clamping. None of the precision faces are ground. Grinding sets up surface stresses due to compression of the grain structure and heat effect. A time lapse of at least several days is allowed between rough and final machining.

By rigorously enforcing recommended procedures from start to finish of the manufacturing cycle it has been shown that the maximum instability that can occur will not exceed $.10 \times 10^{-6}$ inch/inch/year (Reference #2). This stability is quite remarkable when compared to data developed by the National Bureau of Standards in an evaluation of experimental gage block materials. In that study it was shown that a hardenable tool steel (T-15) (Reference #3) prepared and stabilized under laboratory conditions showed a growth rate of $.19 \times 10^{-6}$ inch/inch/year and a ceramic gage block (Reference #4) made of solid aluminum oxide showed a growth rate in excess of $.30 \times 10^{-6}$ inch/inch/year.

A disadvantage of Meehanite is the need to protect it against corrosion, without disturbing the finish which may have been applied to its surfaces.

G 3 Granite

Black Granite (Reference #5), which is a hard composite igneous rock, Diabase, is generally used in surface plates and for making precision parallels for machine shop work. Granite surface plates and table came into use shortly after the Second World War. When first introduced, it was thought that they would be very stable and

capable of being worked to very high accuracies for use as reference surfaces.

Physical Properties

Modulus of Elasticity (psi)	12×10^6
Density (#/in^3)	.10
Thermal Conductivity (BTU/Hr/Sq Ft/inch thick/°F)	12.0
Coefficient of Thermal Expansion	3.1×10^{-6}

One of the desirable characteristics of this material when used as a surface plate is that it is impossible to raise a "burr" on it. Granite will chip, which from the short term point of view is preferable to "burring". A characteristic of a granite surface plate is that "slight day to day variations occur in the surface of the plate that cannot be accounted for. These variations prove to be somewhat larger than those found in similar sizes on a fine grained cast iron plate." (Reference #6)

In addition, granite exhibits definite hygroscopic characteristics. Local growth can be detected from contact with the palm of an operator's hand. Because of the porosity of the surface, it is appreciably more difficult to clean and maintain than a comparable metallic plate.

A practical consideration in the day to day utilization of a granite measuring stage with a metallic film chip holder and glass platen is the markedly low thermal conductivity of granite. The stabilization time required during any shift in the ambient temperature is appreciably longer than for a comparable metal measuring stage. It is extremely difficult to prevent the formation of thermal gradients in the equipment. These gradients will result in a loss of accuracy.

Granite, so far as is known, has never been worked, for industrial applications, in anything but slab form. The configuration in an equipment as complex as this, comprising both a measuring stage and an optical readout frame, could not be accomplished exclusively in granite. In any composite design, (i.e., granite stage, metallic frame) the design parameters would be appreciably complicated because of the marked differential in thermal expansion coefficients. In addition, standard machining practices are not applicable to granite. Consequently, it would be difficult to achieve the basic physical interconnection between a metal frame and granite base.

G 4 Casting Alloy AISI 410

Casting Alloy AISI 410 is the basic hardenable martensitic stainless alloy and can be heat treated to obtain high strength properties. This steel exhibits good corrosion resistance whether heat treated or not.

Physical Properties

Tensile Strength (psi)	190,000 (when drawn at 600°F)
Modulus of Elasticity (psi)	31×10^6
Brinell Hardness	390 (when drawn at 600°F)
Coefficient of Thermal Expansion from 32°F to 1200°F (per degree F)	6.5×10^{-6}

Several studies have been performed on the temporal dimensional stability of the wrought version of AISI 410. A test block was STAT hardened to [redacted] "C" 41 using a following heat treat cycle. It was heated to 1800°F and held one-half hour, oil quenched, then drawn to 600°F, held for one hour, and air cooled. When tested, this block exhibited a change of dimension of 5×10^{-6} inch/inch/year (Reference #7). A similar study on an annealed 410 stainless steel,

case hardened by nitriding, stress relieved at 975°F for 3 hours and then lapped to size showed an instability less than $.1 \times 10^{-6}$ inch/inch/year (Reference #8). It is obvious that the heat treatment of the first specimen introduced stresses that contributed appreciably to the subsequent growth characteristics of the material. It should be pointed out that the foregoing data applies to the wrought version of AISI 410. Although the cast version is similarly alloyed, it is not safe to assume that the same degree of stability can be obtained. The retention of some casting stresses, regardless of the effectiveness of subsequent heat treat cycles, precludes this possibility. Also the forging and/or rolling cycle experienced by wrought stock orients and refines the grain structure, producing a beneficial or stabilizing effect.

In the course of previous programs, experience has been obtained regarding the castability of AISI 410 versus a Meehanite Metal. It has been appreciably more difficult to obtain a sound casting in the 410. The cost to pour in 410 is approximately $2.00/pound versus $0.20/pound for Meehanite. The follow-on machining costs are comparable.

G 5 Conclusions

Each of the three materials discussed above have specific characteristics desirable in a measuring engine. The resistance to corrosion exhibited by AISI 410 and the service ruggedness of granite plates are desirable characteristics.

The ultimate factor, however, must be the contribution the material makes in assuring compliance with the intended end use of the equipment. This does not simply apply to the equipment as delivered but rather to the broader consideration of the equipment function during its useful life. This function, in terms of a high precision measuring machine, is absolute accuracy and repeatability.

The first and primary requisite is that the material be capable of fabrication to micro-inch tolerances and that it be temporally stable. The preponderance of data indicates a choice of a Type GA Meehanite Metal.

Such corollary requirements as good damping characteristics, simplicity of fabrication, ease of maintenance, ready reproducibility are established criteria for the Type G. A. Meehanite.

The fact that this equipment will function in a controlled environment simplifies the problem of corrosion resistance. Additional data will be developed in this area.

List of References

1. Dimensional Stability of Castings by D. M. P. Scott, G. I. Mech. E., Grad I. Prod E. The International Meehanite Metal Co. Ltd, Reigate, Surrey.
2. Measurements Made at National Physical Laboratory, Meehanite Type GA sample - Ref. - "Handbook of Meehanite Metal - Bulletin 49 Revised (1963)".
3. Gage Blocks of Superior Stability II; Fully Hardened Steels, Trans. ASM, 57 3 (1964), by Myerson, R. R. & Pennington, W. A.
4. Gage Blocks of Superior Stability III; the attainment of ultra stability Trans. ASM 57 164 (1964).
5. Materials Handbook, Eighth Edition, by George S. Brady .
6. Engineering Metrology, Second Edition, K. J. Hume. B. Sc., M. I. Mech E. M. I. Prod. E.
7. A review of Dimensional Instability in Metals, Defense Metals Information Center, Battelle Memorial Institute, Columbus 1, Ohio.
8. The Temporal Dimensional Stability of Surface Hardened Steel by Myerson, M. R., Research National Bureau of Standards.